CrIS CHART Retrieval Algorithm ATBD

Contributions by:

J. Susskind NASA GSFC, J. Blaisdell SAIC/NASA GSFC,
L. Kouvaris SAIC/NASA GSFC, and L. Iredell, SAIC/NASA GSFC

December 2017

Version 1.0

Table of Contents

Acronyms 5
Introduction 8
1. CrIS Instrument and Overview of the Retrieval Methodology 10
1.1 Steps in the retrieval algorithms 13
1.1.1 Level-1B 13
1.1.2 MW-Only Retrieval 14
1.1.3 Neural-Net Initial Guess 14
1.1.4 Other Components of First Guess 14
1.1.5 IR/MW Level-2 Retrieval 15
1.1.6 Local Angle Correction 16
2. Channels and Functions Used in Different Processing Steps 16
2.1 Cloud Clearing and Temperature Profile Retrieval 17
2.2 Surface Skin Temperature and Shortwave Spectral Emissivity Retrievals 17
2.3 Surface Longwave Emissivity 18
2.4 Constituent Profile Retrievals 19
3. Error Estimates and QC Flags 19
3.1 Temperature Profile Quality Control 19
3.2 Water Vapor Profile Quality Control 20
3.3 Surface Skin Temperature Quality Control 20
3.3.1 Ocean Surface Skin Temperature 20
3.3.2 Land Surface Skin Temperature 20
3.4 Cloud Parameters and OLR 21
3.5 The Fundamental Level-3 Test Used for Most Geophysical Parameters 21
3.6 Error Estimates and Quality Control for Clear Column Radiances $\hat{R}_i$ 22
4. Single Day Comparison of Quality Controlled CrIS and AIRS Retrievals 22
4.1 *T(p)* and $q(p)$ Retrieval Accuracy as a Function of Yield 23
4.2 Ocean Surface Skin Temperature T_s and Surface Spectral Emissivity ε_ν 27
4.3 Land Surface Temperature and Spectral Emissivity 30

4.4 Retrieval of Cloud Fraction $\alpha\varepsilon$ and Cloud Top Pressure p_c 32
4.5 OLR and Clear Sky OLR 34
4.5.1 OLR 34
4.5.2 OLR_{CLR} 35
4.6 Total Ozone 36
4.7 Clear Column Radiances 37
5. Comparison of CrIS/ATMS and AIRS Monthly Mean Products 39
5.1 Comparison of Select CrIS and AIRS Monthly Mean Products with Each Other 39
5.2 Comparison of Select CrIS and AIRS Monthly Mean Products with those of Other Measures of the same Geophysical Parameters 42
5.2.1 OLR 42
5.2.2 Total ozone 43
6. Implications toward meeting the goal of the research 44
References 45

List of Figures

Figure 1 AIRS and CrIS channels used in different retrieval steps 17
Figure 2 Temperature Profile Plots 24
Figure 3 500 mb Temperature 25
Figure 4 Water Profile Plots 26
Figure 5 Total Precipitable Water 27
Figure 6 Surface Skin Temperature Histogram 50°N to 50°S 28
Figure 7 Ocean Surface Skin Temperature 50°N to 50°S 29
Figure 8 Ocean Surface Emissivity as a Function of Zenith Angle 30
Figure 9 Surface Skin Temperature 31
Figure 10 Land Surface Spectral Emissivity 32
Figure 11 Cloud Parameters 34
Figure 12 OLR 35

Figure 13 Clear Sky OLR 36
Figure 14 Total Ozone 37
Figure 15 Cloud Cleared Radiances 38

Monthly Mean Figures for July 2015:

Figure 16 Surface Temperature and Total Precipitable Water 40
Figure 17 500 mb Temperature and 300 mb Temperature 41
Figure 18 Clouds and Clear Sky OLR 42
Figure 19 OLR 43
Figure 20 Total Ozone 44

Acronyms

AIRS	**A**tmospheric **I**nfra**r**ed **S**ounder
AIRS Only	**AIRS IR Only**
AO	**AIRS Only**
AMSU	**A**dvanced **M**icrowave **S**ounding **U**nit
ATBD	**A**lgorithm **T**heoretical **B**asis **D**ocument
ATMS	**A**dvanced **T**echnology **M**icrowave **S**ounder
ATOVS	**A**dvanced **TOVS**
CDR	**C**limate **D**ata **R**ecord
CHART	**C**limate **H**eritage **AIRS R**etrieval **T**echnique
CrIMSS	**Cr**oss-track **I**nfrared and **M**icrowave **S**ounding **S**uite
CrIS	**Cr**oss-track **I**nfrared **S**ounder
EDR	**E**nvironmental **D**ata **R**ecord
EDOS	**E**OS **D**ata and **O**perations **S**ystem
EOS	**E**arth **O**bserving **S**ystem
EOSDIS	**EOS D**ata and **I**nformation **S**ystem
FOR	**F**ield **o**f **R**egard
FOV	**F**ield **o**f **V**iew
FSR	**F**ull **S**pectrum **R**esolution
FWHM	**F**ull **W**idth at **H**alf **M**aximum
GCM	**G**eneral **C**irculation **M**odel
GES DISC	**G**oddard **E**arth **S**ciences **D**ata and Information **S**ervices **C**enter
GFS	**G**lobal **F**orecast **S**ystem
GSFC	**G**oddard **S**pace **F**light **C**enter
HSB	**H**umidity **S**ounder for **B**razil
IR	**I**nfra**r**ed
IR Only	**AIRS IR Only** or **CrIS IR Only**
JPL	**J**et **P**ropulsion **L**aboratory
JPSS	**J**oint **P**olar **S**atellite **S**ystem

L0	**L**evel-**0** (unprocessed instrument data at full resolution)
L1A	**L**evel-**1A** (unprocessed instrument data at full resolution, time-referenced, and annotated with ancillary information, including radiometric and geometric calibration coefficients appended but not applied to L0 data)
L1B	**L**evel-**1B** (L1A data processed to sensor units)
L2	**L**evel-**2** (Retrieved geophysical variables)
L3	**L**evel-**3** (Variables mapped on uniform grid scales with completeness and consistency)
L4	**L**evel-**4** (Model output or results from analyses of variables derived from multiple measurements)
LST	**L**and **S**urface **T**emperature
MHS	**M**icrowave **H**umidity **S**ounder
MIT	**M**assachusetts **I**nstitute of **T**echnology
MODIS	**Mo**derate **R**esolution **I**maging **S**pectrometer
MSU	**M**icrowave **S**ounding **U**nit
MW	**M**icro**w**ave
NASA	**N**ational **A**eronautics and **S**pace **A**dministration
NEDT	**N**oise-**e**quivalent **d**elta-**T**
NOAA	**N**ational **O**ceanic and **A**tmospheric **A**dministration
NPOESS	**N**ational **P**olar-orbiting **O**perational **E**nvironmental **S**atellite **S**ystem
NPP	**NPOESS P**reparatory **P**roject
NSR	**N**ormal **S**pectrum **R**esolution
OLR	**O**utgoing **L**ongwave **R**adiation
OMPS	**O**zone **M**apping and **P**rofiling **S**uite
OPD	**O**ptical **P**ath **D**ifference
POES	**P**olar-orbiting **O**perational **E**nvironmental **S**atellite
QC	**Q**uality **c**ontrol
RDR	**R**aw **D**ata **R**ecord
RTA	**R**apid **T**ransmittance **A**lgorithm
SCC/NN	**S**tochastic **C**loud **C**learing/**N**eural **N**etwork

SDR	**S**ensor **D**ata **R**ecord
SNPP	**S**uomi **N**ational **P**olar **P**artnership
TIROS	**T**elevision **I**nfra**r**ed **O**bservation **S**atellite
TOVS	**T**IROS **O**perational **V**ertical **S**ounder
V6	**V**ersion-**6**
V7	**V**ersion-**7**

Introduction

AIRS (Atmospheric Infrared Sounder) is a high spectral resolution IR grating spectrometer flying on EOS Aqua generating data products operationally from September 2002 through current time using the AIRS Science Team Version-6 retrieval algorithm. AIRS Version-7 is significantly improved over Version-6 and is expected to become operational in early 2018, and will to generate AIRS products for its entire data record extending into the future. AIRS is accompanied by AMSU (Advanced Microwave Sounding Unit), a microwave radiometer. CrIS (Cross-Track Infrared Sounder and Advanced Technology Microwave Sounder) is a high spectral resolution IR interferometer with spatial and spectral characteristics similar to those of AIRS. It is accompanied by ATMS (Advanced Technology Microwave Sounder), a microwave radiometer. CrIS/ATMS is flying on SNPP and was recently launched on NOAA-20.

The objective of this research is to develop and implement an algorithm to analyze a long term data record of CrIS/ATMS observations so as to produce monthly mean gridded Level-3 products which are consistent with, and will serve as a seamless follow on to, those of AIRS Version-7. We feel the best way to achieve this result is to analyze CrIS/ATMS data using retrieval and Quality Control (QC) methodologies which are scientifically equivalent to those used in AIRS Version-7. We developed and implemented a single retrieval program that uses as input either AIRS/AMSU or CrIS/ATMS radiance observations, and has appropriate switches that take into account the spectral and radiometric differences between CrIS and AIRS. Our methodology is called CHART (Climate Heritage AIRS Retrieval Technique). Our measure of success is the level of agreement between CrIS CHART and AIRS Version-7 monthly mean products for months in common, and even more importantly, the level of agreement between interannual differences of CrIS and AIRS monthly mean products.

The CrIS and ATMS were launched on Suomi-NPP in October 2011 as part of a sequence of Low Earth Orbiting satellite missions under the JPSS. CrIS and ATMS are advanced Infrared and Microwave atmospheric sounders that were designed as follow-ons to the AIRS and AMSU sounders flying on EOS Aqua. CrIS is an interferometer generally with similar spectral coverage and noise characteristics to those of AIRS. CrIS contains three spectral bands: band 1 covering 650 cm^{-1} to 1095 cm^{-1}; band 2 covering 1210 cm^{-1} to 1750 cm^{-1}; and band 3 covering 2155 cm^{-1} to 2550 cm^{-1}. Unlike a grating instrument, like AIRS, which is characterized by a roughly constant resolving power, the “spectral resolution” of an interferometer is constant within a band, and it depends on the maximum Optical Path Difference (OPD) L of that band. L was originally set at 0.8 cm, 0.4 cm, and 0.2 cm for CrIS bands 1, 2, and 3, respectively. CrIS measurements with L=0.8 cm (FSR) for all bands have been down linked since early

December 2014. The spectral sampling interval of an interferometer is given by ½ *L*, corresponding to 0.625 cm^{-1} in band 1, 1.25 cm^{-1} in band 2, and 2.5 cm^{-1} in band 3 (NSR) in the early part of the NPP mission. The FWHM or "spectral resolution" of an interferometer depends on the type of apodization used to transform the interferogram into the radiance domain. Unlike AIRS, the CrIS spectral response functions have sidelobes which are apodization dependent. Barnet et al. (2000) and co-workers have shown that use of a Hamming apodization function provides an optimum balance between minimizing the FWHM of the central lobe of the spectral response function on the one hand, and the size of the spectral side lobes on the other. Using Hamming apodization, the FWHM of the central lobe is given by 0.9/*L*, which originally corresponded to 1.125 cm^{-1}, 2.25 cm^{-1}, and 4.5 cm^{-1} for bands 1 to 3 respectively. Both the spectral sampling and "spectral resolution" of the original CrIS channels are roughly twice as coarse as those of corresponding AIRS channels. The spectral radiometric noise characteristics of CrIS channels are somewhat similar to those of AIRS, but are lower than AIRS at lower frequencies and higher than those of AIRS at higher frequencies. The goal of this research is to generate monthly mean L3 gridded products from CrIS/ATMS which will be compatible with, and of comparable quality to, those generated operationally using AIRS/AMSU data. AIRS Verion-7 retrievals should become operational in the near future. In order to achieve this goal, it is essential that CrIS/ATMS radiances be analyzed using a retrieval algorithm scientifically analogous to that of AIRS V7.

The basic cloud clearing and retrieval methodologies used in the CrIS CHART retrieval algorithm, including the definition and derivation of Jacobians, the channel noise covariance matrix, and the use of constraints including the background term, are essentially identical to those of AIRS Version-7 and previous AIRS Science Team retrieval algorithms described in Susskind et al. (2003, 2006, 2011, and 2014). ATBDs for the entire L1 through L2 AIRS processing are located at https://eospso.gsfc.nasa.gov/atbd-category/37 Susskind et al. (2006) introduced a Quality Control (QC) concept that generated different QC flags for a given profile as a function of height, and also had separate QC flags related to surface skin temperature. The AIRS Science Team Version-5 retrieval algorithm (Susskind et al., 2011) contained many further improvements. The most important improvement in retrieval methodology was found in the set of channels used to retrieve the atmospheric temperature profile. In addition, new methodology was described to generate profile-by-profile, level-by-level, error estimates of temperature profile and to use them for level-by-level QC of the atmospheric temperature profile. The AIRS Version-6 retrieval algorithm described in Susskind et al. (2014) contains many further improvements in retrieval methodology. Foremost among these is a major improvement in the ability to determine surface skin temperature and surface spectral emissivity from AIRS observations. There have also been significant improvements to the QC methodology used for different geophysical parameters,

the methodology used to generate first guesses for atmospheric and surface parameters, and the methodology used to determine cloud parameters and derive OLR from the AIRS/AMSU observations. CHART uses analogous retrieval and QC methodology for CrIS/ATMS. Improvements to the retrieval and QC methodology since Version-6 are discussed in this ATBD. The production Version-6 had an "AIRS Only" processing capability which utilizes only AIRS observations and produces results only slightly degraded from those obtained utilizing both AIRS and AMSU observations. This "AIRS Only" capability is an important backup processing mode because some channels of AMSU-A degraded to the point of being turned off in September of 2016. A corresponding CrIS Only processing system is currently under development for use if the ATMS fails.

1. CrIS Instrument and Overview of the Retrieval Methodology

The CrIS/ATMS suite was designed as a follow-on sensor suite to the AIRS/AMSU/HSB sensors launched on Aqua in 2002. Because the instrument specifications and purpose are similar, CHART uses essentially the same retrieval algorithm and QC methodology for the analysis of CrIS and AIRS data, with appropriate adaptations to the characteristics of each instrument. The fact that CrIS is an interferometer rather than a grating spectrometer like AIRS has some consequences within the details of the algorithm, but scientifically, the approach taken is equivalent. ATMS also differs from the AMSU in significant ways, but which are less important to the overall retrieval methodology.

Besides similarity of instruments for building a long-term data set, similarity of the retrieval algorithm is essential to establish continuity. The CHART algorithm therefore makes maximal use of the AIRS/AMSU software, with allowances for consequences of the instrumental differences. The most important computational difference between CrIS and AIRS in the infrared is that radiances in CrIS spectral channels are transformed from an interferogram, and therefore, channel noises are correlated with each other. The AIRS Science Team retrieval algorithm, on which CHART is based, uses to great advantage the fact that localized spectral channels are often sensitive to absorption and emission by primarily one or a few atmospheric components, enabling the retrieval to be done in a sequential manner. The AIRS algorithm also relies entirely on the Rapid Transmittance Algorithm (RTA) concept of estimating the forward radiance seen from an atmospheric state, which works best for localized spectral channels. Radiances using unapodized CrIS spectra are sensitive to absorption and emission in broad spectral regions, and are thus less suitable for the CHART algorithm approach of sequential solution of different geophysical parameters using select channel radiances for each.

The CrIS channel response functions used in CHART are obtained via Hamming

apodization of the CrIS interferogram. The Hamming apodization results in considerable similarity of CrIS spectral response function to those of AIRS. Hamming apodization was therefore chosen by Larrabee Strow as the most suitable for the RTA for the CHART algorithm approach (Strow, et al., 1998). The Hamming apodization minimizes negative side lobes in the transform and has been shown to be reversible and computationally efficient (Barnet, et al., 2000). Using the Hamming apodization, there is correlated channel noise in Hamming apodized channels radiances. This correlated noise is added to the channel-by-channel noise covariance matrix in each retrieval step. Individual channels can then be used in the retrieval steps in an analogous way as they are used for AIRS.

There are also significant scientific differences between AIRS and CrIS in that the spectral ranges are different as well as the channel noise. The spectral gaps between the bands (see Figure 1) also lie in different places for the two instruments, providing somewhat different information content in the two instruments. The high redundancy of the information in the infrared spectrum mitigates the impact of the spectral differences, but it is notable that CrIS contains the spectral region around 1700 cm^{-1}, with additional water band information, as compared to AIRS, and AIRS has spectral coverage beyond 2550 cm^{-1}. Figure 1 shows that surface skin temperature is determined in both instruments using shortwave channels, which extend further in AIRS than in CrIS. This limitation on CrIS might serve to degrade the accuracy of CrIS surface skin temperatures under the same conditions. In addition, there are differences in the effective noise on the channels. CrIS has lower noise than AIRS in the long-wave band and higher noise in the short-wave band. This affects the relative weighting of channels as used in the various retrieval steps.

The differences between ATMS and the AMSU/HSB suite are also important. AMSU/HSB suffered from loss of channels (HSB early in the mission, and AMSU channels 4, then 5, then 1 and 2, becoming unusable after a period of many years) while ATMS has suffered from data dropouts resulting from the engineering need to reverse the scan direction to preserve the motor functionality. In the retrieval algorithm discussion in this document, the differences (other than data availability) are encapsulated in the microwave RTAs provided by Philip Rosenkranz of MIT (Rosenkranz, 2000).

Fundamental to CHART and all versions of the AIRS Science Team retrieval algorithm is the generation of clear column radiances for each channel i, $\hat{R}_i$, which are derived products. $\hat{R}_i$ represents the radiance channel i would have seen if the entire single 3x3 Field of Regard (FOR) on which a retrieval is performed were cloud free. $\hat{R}_i$ is determined for each channel as a linear combination of the observed radiances of that channel in each of the 9 Fields of View (FOV's) contained within the FOR, using coefficients that are channel independent (Susskind et al., 2003). The retrieved geophysical state X is subsequently

determined which, when substituted into the RTA (Strow et al., 1998), generates an ensemble of computed radiances $R_i(X)$ which are consistent with $\hat{R}_i$ for those channels i used in the determination of X. Cloud-clearing theory (Chahine, 1974, 1977) says that to achieve the best results under more stressing cloud conditions, longwave channels sensitive to cloud contamination should be used only in the determination of the coefficients used in the generation of clear column radiances for all channels, and not be used for sounding purposes. Susskind et al. (2011) describes the AIRS Version-5 retrieval methodology, in which tropospheric sounding 15 μm CO_2 radiance observations R_i were used only in the derivation of the cloud clearing coefficients, while temperature profiles were derived using $\hat{R}_i$ in the 4.3 μm CO_2 band, as well as in some stratospheric sounding 15 μm CO_2 channels that do not see clouds. This approach allowed for the retrieval of accurate Quality Controlled values of $\hat{R}_i$ and the temperature profile, *T(p)*, under more stressing cloud conditions than was achievable in previous versions. The AIRS Version-5 processing system also contained methodology to provide accurate case-by-case level-by-level error estimates for retrieved geophysical parameters as well as for channel-by-channel clear column radiances. Thresholds of these error estimates were used for Quality Control.

The AIRS Version-6 retrieval algorithm had further significant advances over Version-5. The basic theoretical approach used in Version-6 to analyze AIRS/AMSU and CrIS/ATMS data is very similar to that used in Version-5 with one major exception. As in Version-5, the coefficients used for generation of clear column radiances $\hat{R}_i$ for all channels are determined using observed radiances only in longwave 15 μm and 11 μm channels. In Version-5, tropospheric temperatures were retrieved using only $\hat{R}_i$ in the shortwave 4.2 μm CO_2 channels, although surface skin temperature was retrieved simultaneously, along with surface spectral emissivity ε_ν and bi-directional reflectance, using $\hat{R}_i$ both in the longwave 8 - 12 μm window region as well as in the shortwave 4.0 μm – 3.76 μm window region. In Version-6, only window observations in the shortwave window region are used to simultaneously determine surface skin temperatures along with shortwave surface spectral emissivities and surface bi-directional reflectance. Longwave surface spectral emissivity is retrieved in a subsequent step using $\hat{R}_i$ in channels in the longwave window region. Another significant improvement found in Version-6 is the use of an initial guess X^o generated by using Neural-Net methodology (Tao et al., 2011, Blackwell, 2011) in place of the previously used regression approach. These two modifications have resulted in significant improvement in the ability to obtain both accurate temperature profiles and surface skin temperatures under more stressing partial cloud cover conditions. They also allow for the accurate determination of surface air temperatures.

In the Version-7 system, some tropospheric sounding 15 μm channels are used in the temperature profile retrieval on a case-by-case basis. These channels are used only if the cloud correction to $\hat{R}_i$ is less than five degrees in Brightness Temperature. This provides additional *T(p)* information in clearer cases without introducing much cloud clearing noise.

1.1 Steps in the retrieval algorithm

1.1.1 Level-1B

The CrIS/ATMS Level-1B MW data is described by Lambrigtsen (2014) and the IR data by Revercomb and Strow (2017) in their ATBD documents. Lambrigtsen describes the algorithms as very similar to those that have been developed by NOAA and NASA for the AMSU-A and AMSU-B instruments, which have flown since 1998 (NOAA) and 2002 (NASA), respectively. Details are based on the current Aqua AMSU-A/HSB implementation. The primary input to the L1B software is L0 data, which is composed of raw CCSDS packets as received from the spacecraft, together with added metadata. L0 data is produced and distributed by EDOS, and is equivalent to RDR data in the operational JPSS processing system. The MW and IR L1B software generates L1A and L1B product files. The L1A product contains unpacked spacecraft telemetry data that has been granulated and geolocated, as well as quality flags and metadata. There is no equivalent to the CrIS L1A product in the current operational JPSS processing system. The L1B product contains calibrated spectra, together with geolocation information, quality flags, diagnostic information and metadata. L1B is equivalent to SDRs in the current operational processing system. The L1B product is used as input to L2 processing (equivalent to EDRs in the current operational processing system).

The CHART CrIMSS Level-2 processing starts with CrIMSS L1B data from the GES DISC which is made available in NetCDF4 format for the CrIS and ATMS instruments. The CrIS data is available in two spectral resolutions: Normal Spectral Resolution (NSR) and Full Spectral Resolution (FSR). At present we only run retrievals using the NSR data. The L1B data is run through a preprocessor that locates the nearest ATMS footprint to a given CrIS footprint and outputs files of CrIS and ATMS radiances and brightness temperatures that are matched together as best as possible in time and geographic location (Gambacorta, 2013). Our only deviation from Gambacorta (2013) is that we use 7 MW hinge points for the characterization of the MW surface spectral emissivities, whereas Gambacorta uses 13 for the surface characterization. In addition, the preprocessor outputs a file containing the atmospheric state from GFS data, interpolated in time and space to the CrIS footprint. This GFS file is only used for the surface pressure as a boundary condition in the calculation of expected radiances for a given state. These three files, CrIS, ATMS, and GFS, are the main inputs to the CrIS retrieval code.

1.1.2 MW Only Retrieval

The AMSU/HSB microwave retrieval step was developed by Phil Rosenkranz for the AIRS Science Team, and he subsequently modified the forward and retrieval algorithms to accommodate the ATMS channels and polarizations. This algorithm is described in the AIRS ATBD and in Gambacorta (2013), and references therein. In the CHART system, the only outputs of this retrieval step which are used in subsequent steps are the surface classification, the liquid water determination, and the microwave surface spectral emissivity.

1.1.3 Neural-Net Initial Guess

Once the preprocessor has assembled radiance data and associated geolocation data and forecast surface pressure into groups of nine IR spots and one associated MW spot, the Stochastic Cloud Clearing/Neural Network (SCC/NN) step is called. The SCC/NN software and coefficient files were provided by MIT/Lincoln Labs. They were developed by William Blackwell and Adam Milstein, following the methods outlined in Blackwell (2005) and an updated validation description provided by Milstein and Blackwell (2016). The training coefficients were derived from matching observed radiances with selected collocated ECMWF analyses during the 2013-2014 period. These coefficients are applied profile-by-profile for all time periods. Milstein and Blackwell stratify coefficients into four seasons, three latitude bands, ascending vs. descending orbits, and nine surface types: ocean, frozen, and seven land types which depend only on forecast surface pressure coming from the GFS.

The SCC/NN software returns a temperature profile on 100 levels, a water profile on 100 levels, and a surface skin temperature. These parameters are saved and passed along to the physical retrieval as a first guess state.

The neural network step generally reports success, with error flags for unexpected detection of sea ice or missing input data.

1.1.4 Other Components of the First Guess

Besides the SCC/NN temperature profile, water profile, and surface skin temperature, other parameters are needed for the complete atmospheric state needed for use in the RTA. The CO_2 first guess is a linear ramp in time derived by Larrabee Strow for the AIRS Team and implemented as in AIRS Version-6. The Version-7 ozone profile guess is derived from a monthly mean zonally averaged spatial climatology developed by Gordon Labow for the AIRS Science Team. This climatology is based on ozonesondes. It also includes distinct

profiles for ozone hole cases in which the profile is sharply different from normal conditions. In non-ozone hole cases, we adjust the first guess ozone by stretching or shrinking the shape of the Labow O_3 profile from 50mb down to the tropopause according to the tropopause height determined from the neural net input temperature profile. The *CO* first guess used in Version-7 is Version-4 of the climatology developed for the MOPITT instrument, as was used in AIRS Version-6. The CH_4 first guess is also that used by AIRS Version-6, developed by Xiaozhen Xiong from CMDL and HALOE data. Identical trace gas guesses are also used in AIRS Version-7.

The surface IR emissivity first guess follows the AIRS Version-6 methodology. Over ocean, the AIRS team model due to Evan Fishbein is used for surface emissivity. Over land, a one year spatial climatology, based on MODIS observations for the year 2008, is used. The MODIS observations are expanded to the CrIS spectrum using the method of Seemann, et al. (2007).

1.1.5 IR/MW Level-2 Retrieval

Retrievals of all geophysical parameters are physically based and represent states $X_{j,c}$ determined for case *c* that best match the set of clear column radiances $\hat{R}_{i,c}$ for the subset of channels i used in the retrieval process for that step. Retrievals of geophysical parameters are performed sequentially, that is, only a subset of the geophysical parameters within the state $X_{j,}$ is modified from that of the incoming state X_j^0 in a given step. In the case of IR Only retrievals, a GCM Forecast is used to determine the surface class of ocean, land, or ice, which would otherwise have been determined in the microwave retrieval step.

Susskind et al. (2011) describes the steps of the AIRS Version-5 physical retrieval process, while Susskind et al. (2014) updated the description for the Version-6 system, which have not changed for Version-7. The steps are summarized here:

A SCC/NN start-up procedure is used to generate the initial state X^o. Initial clear column radiances $\hat{R}_i^0$ are generated for all channels i using a case dependent fit of cloud clearing (CC) coefficients consistent with observed radiances in the ensemble of cloud clearing channels. The coefficients are somewhat dependent on the initial state X^o, which in general is very accurate for the Neural-Net, even in very cloudy cases. The state X^o is also used as the initial guess to the physical retrieval process in which IR/MW observations are used to retrieve: *a*) shortwave reflectance in daytime cases; *b*) surface skin temperature, surface spectral emissivity and refined surface bi-directional reflectance of solar radiation; *c*) atmospheric temperature profile; *d*) atmospheric moisture profile; *e*) longwave spectral emissivity; *f*) atmospheric ozone profile; *g*) atmospheric CO profile; *h*) atmospheric CH_4

profile; and *i*) cloud properties and OLR. These steps are done sequentially, solving only for the variables to be determined in each retrieval step while using previously determined variables as fixed, with an appropriate uncertainty attached to them that is accounted for in the channel noise covariance matrix used in that step (Susskind et al., 2003). The objective in each step (*a*-*h*) was to find solutions which best match $\hat{R}_i$ for the subset of channels selected for use in that step, bearing in mind the channel noise covariance matrix. Steps *a*-*h* were ordered so as to allow for selection of channels in each step which are primarily sensitive to variables to be determined in that step or determined in a previous step, and are relatively insensitive to other parameters. Separation of the problem in this manner allows for the problem in each step to be made as linear as possible. Step i is performed last using a selected set of the observed radiances R_i and determines cloud parameters which are consistent with the surface and atmospheric conditions that have been determined previously.

Only shortwave window channels are used in retrieval step *b*) which simultaneously determines T_s, $\varepsilon_{sw}(\nu)$ and $\rho_{sw}(\nu)$. The longwave surface spectral emissivity $\varepsilon_{lw}(\nu)$ is solved for in step e) using only channels in the longwave window spectral region. This step is performed after the humidity profile retrieval step has been performed because longwave window radiances can be very sensitive to the amount of atmospheric water vapor. The steps used in the IR-only algorithm are otherwise identical, but no microwave observations are used in the physical retrieval process, nor in the SCC/NN start-up procedure.

1.1.6 Local Angle Correction

All versions of the AIRS Science Team retrieval algorithm use a local angle correction within the field of regard to correct the nine radiances to the values which would have been observed if all nine AIRS spots had been at the viewing angle of the center spot. At this time no similar correction algorithm has been developed, for CrIS. The rotation of the CrIS field of view with scan angle makes the problem more difficult than for AIRS as much more modeling data would be required. Studies with AIRS have shown the effect of the lack of a CrIS zenith angle correction is quite small, so this is deferred until later versions.

2. Channels and Functions Used in Different Processing Steps

Figure 1 shows a typical AIRS and CrIS cloud free brightness temperature spectrum and includes the channels used for each instrument for cloud clearing (CC), as well as in each of the subsequent steps of the physical retrieval algorithm. The channels used in different retrieval steps are described below.

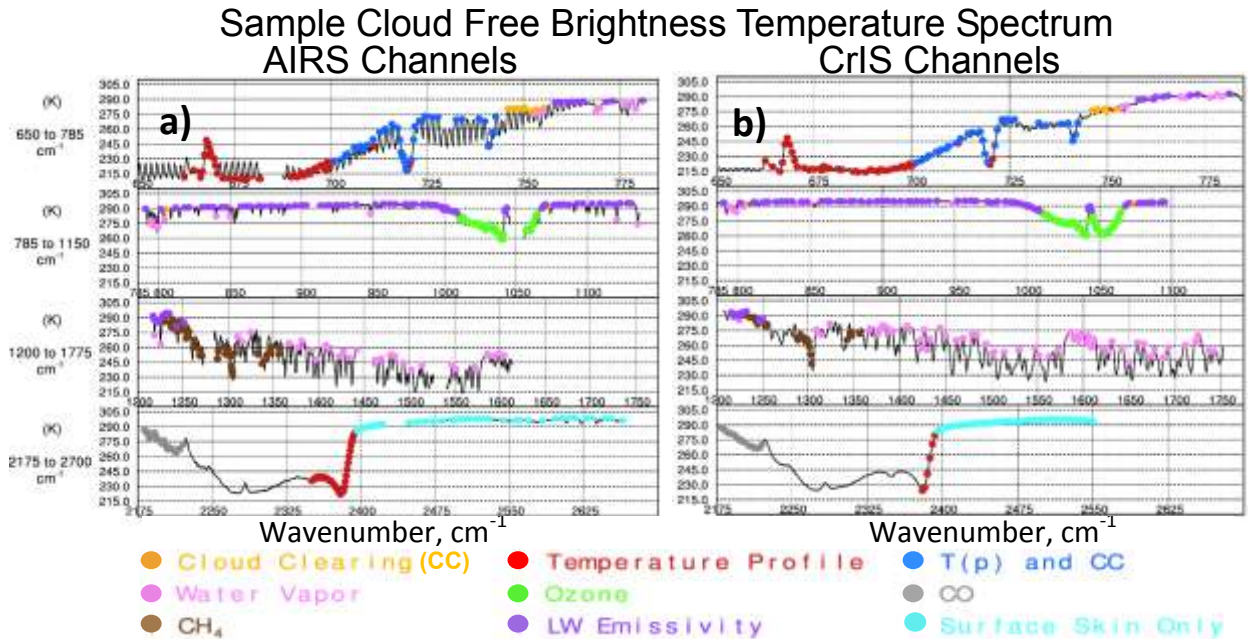

Figure 1. AIRS and CrIS channels used in different retrieval steps

2.1 Cloud clearing and temperature profile retrieval

Following cloud clearing theory (Chahine, 1974, 1977) coefficients needed to generate clear column radiances for all channels are determined using observations in longwave channels, ranging from 701 cm^{-1} to 1228 cm^{-1}, which we show in yellow in Figure 1. The methodology used to determine the cloud clearing coefficients is the same as that described in Susskind, et al. (2003). The cloud clearing channels are also the ones used in a subsequent cloud parameter retrieval step. The temperature profile retrieval step uses channels between 2380 cm^{-1} and 2398 cm^{-1} that are sensitive to both stratospheric and tropospheric temperatures, as well as stratospheric sounding channels between 662 cm^{-1} and 743 cm^{-1} that are not sensitive to cloud contamination. We show these channels in red in Figure 1. The CrIS/ATMS retrieval also uses ATMS channels 7-15 in the temperature profile retrieval.

2.2 Surface skin temperature and shortwave spectral emissivity retrievals

The surface skin temperature retrieval step uses channels between 2395 cm^{-1} and 2550 cm^{-1}, which are shown in light blue in Figure 1, along with the highest frequency channels which are also used in the temperature profile retrieval step. These channels are used to determine T_s simultaneously with surface shortwave spectral emissivity, and, during the day, shortwave surface bi-directional reflectance.

Like the AIRS Version-7 retrieval system, CHART uses an improved multiplicative form of the equation to modify the retrieved surface spectral emissivity ε_ν from its initial guess ε_ν^0. We treat the variable to be modified as (1-ε_ν), and write

$$(1-\varepsilon_\nu) = (1-\varepsilon_\nu^0)\left[1+\sum_{k=1}^{kmax} A_k\, F_k(\nu)\right] \quad (1)$$

where F_k are triangular functions of frequency. The equation is written in this form so that $\varepsilon_\nu = \varepsilon_\nu^0$ if all coefficients A_k are equal to 0. A corresponding multiplicative form is also used to modify ρ_ν

$$\rho_\nu = \rho_\nu{}^o[1+\sum_k^1 B_k F_k(\nu)]. \quad (2)$$

For CrIS we set k_{max}=1, while for AIRS we set k_{max} equal to 4, because the AIRS shortwave window extends further than that of CrIS.

$\rho_\nu{}^o$ in equation 2 is initially estimated as being equal to $(1-\varepsilon_\nu{}^o)/\pi$, but then modified in a subsequent step which is performed immediately prior to the shortwave surface parameter retrieval step. In that step, $\rho_\nu{}^o$ is updated in a one parameter physical retrieval step, using the same channels as in the surface parameter retrieval step, according to

$$\rho_\nu{}^o = [(1-\varepsilon^o)/\pi]\,(1+C) \quad (3)$$

where C is a constant which scales $\rho_\nu{}^o$ but does not change its shape. The values of $\rho_\nu{}^o$ shown in Equation 3 are used as the initial guess in Equation 2. Determination of this constant prior to the full surface retrieval step significantly improved the retrieved values of T_s, ε_ν, and ρ_ν determined during daytime.

2.3 Surface longwave emissivity

Surface longwave spectral emissivity is determined using channels between 758 cm^{-1} and 1250 cm^{-1}, which we show in purple in Figure 1. In this step, coefficients of eight longwave emissivity perturbation functions are solved for for both CrIS and AIRS with T_s being held fixed at the value determined from the previous skin temperature retrieval step. The initial guess for surface spectral emissivity in both retrieval steps, ε_ν^0, is set equal to the values found in the AIRS Science Team ocean emissivity model over non-frozen ocean. Over land, ε_ν^0 is set equal to values interpolated from the 1° x 1° monthly mean MODIS Science Team surface spectral emissivity data set for the year 2008. An ice emissivity model is used over frozen cases.

2.4 Constituent profile retrievals

Constituent profile retrievals are performed in separate subsequent steps, each having its own set of channels and functions. Figure 1 shows, in different colors, the channels used in each of these retrieval steps. The $q(p)$ retrieval (pink dots) uses channels in the spectral ranges 753 cm^{-1} to 948 cm^{-1} and 1218 cm^{-1} to 1743 cm^{-1}; the $O_3(p)$ retrieval (green dots) uses channels between 997 cm^{-1} and 1069 cm^{-1}; the $CO(p)$ retrieval (gray dots) uses channels between 2180 cm^{-1} and 2220 cm^{-1}; and the $CH_4(p)$ retrieval (brown dots) uses channels between 1220 cm^{-1} and 1356 cm^{-1}.

3. Error estimates and QC Flags

Each retrieved quantity X has an associated error estimate δX assigned to it. The retrieval system generates empirical error estimates for a number of geophysical parameters, and uses thresholds of these error estimates for Quality Control. There are six distinct matrices for separate use to generate empirical error estimate coefficients. Different coefficients are used under daytime or nighttime conditions, for separate use over 1) non-frozen ocean; 2) non-frozen land; and 3) frozen (ice or snow) cases. Appendix B of Susskind et al. (2011) gives a description of the 16 tests used to provide input parameters into the equations used to generate the case-by-case error estimates coefficients for $T(p)$, $q(p)$, and surface skin temperature. The AIRS Version-6 ATBD further builds upon this. The following sections briefly summarize the use of error estimates for QC purposes for different geophysical parameters. Single day results using the QC procedures described in section 4 are shown in section 5 for April 15, 2016, with references to them incorporated throughout this document.

3.1 Temperature Profile Quality Control

All cases in which the retrieval system converged (about 99% of the cases), are assigned to have highest quality (QC=0) down to at least 30 mb. Two characteristic pressures, *PBest* and *PGood*, are defined analogously to what was described in the Version-6 AIRS ATBD. There are two different sets of error estimate thresholds, Data Assimilation (DA) thresholds, and Climate (Clim) thresholds, which are each defined as a function of *p*. Separate DA and Clim thresholds are defined for each of the six categories mentioned above: day, night, non-frozen ocean, ice and snow covered cases, and land. *PBest* is the lowest pressure at which the error estimate is less than or equal to the pressure dependent DA threshold at that pressure. Pressures lower than or equal to *PBest* are assigned QC=0. *PGood* is the lowest pressure at which the error estimate is less than or equal to the pressure dependent Clim threshold. Cases are flagged as QC=1 between *PBest* and *PGood*. Cases are flagged

as QC=2 beneath *PGood.* Level-3 temperature products at a given pressure include all cases with QC=0 or QC=1. Results of QC'd single day $T(p)$ are shown later in Figure 2.

3.2 Water vapor profile Quality Control

Error estimates for the water vapor profile $\delta q(p)$, and for channel clear-column radiances $\delta \hat{R}_i$, are also computed empirically, but in a different manner from that used to generate δT_s, $\delta T(p)$,δW_{tot} as described in the AIRS Version-6 ATBD. In Version-7, $\delta q(p)$ is written out but is not used for QC purposes. The QC flag for $q(p)$ at pressure *p* in a given profile is set to be the same as that of *T(p)* at that pressure. Single day QC'd $q(p)$ results are shown later in Figure 3.

3.3 Surface skin temperature Quality Control

The use of error estimates for surface parameter Quality Control is somewhat different over non-frozen ocean on the one hand, and over land and frozen ocean on the other hand. These two approaches are described in the next two sections.

3.3.1 Ocean Surface Skin Temperature (SST)

The retrieval system uses the ocean skin temperature error estimate δT_s directly for Quality Control, with separate thresholds ΔT_s^{best} and ΔT_s^{good} used to indicate best quality retrievals (QC=0) and good quality SST retrievals (QC=1). Level-3 products include all cases flagged as either QC=0 or QC=1. We refer to ocean surface skin temperature as sea surface temperature (SST). SST is known quite well from other sources, such as MODIS and ship measurements, and varies slowly in space and time. Therefore, spatial coverage of QC'd SST retrievals is less important. We cannot tolerate a SST error of more than 1K, however. The SST error estimates and Quality flags described in this section are the ones used in the generation of the results shown later in Figures 4 and 5. The Quality Flags for ocean surface spectral emissivities are the same as those used for the ocean surface skin temperature. The ocean surface spectral emissivity results shown in Figure 6 are based on cases with QC=0 or 1.

3.3.2 Land Surface Skin Temperature (LST)

A somewhat different QC approach is used for LST than for SST. Unlike SST, LST varies rapidly in space and time and is not well known from other sources. For this reason, the LST QC methodology is relatively loose, with the goal of getting good spatial coverage. The LST QC procedure flags LST as good (QC=1) if *T(p)* is flagged good down to at least

1.5 km above the surface (see 4.2). In addition, retrieved LST has to be within 7K of the NN LST guess to be flagged as having good quality. An analogous QC approach is also used for frozen ocean cases. Land surface spectral emissivities are given the same flag as LST. Figure 7 shows results of both CrIS and AIRS land surface spectral emissivity using this approach.

3.4 Cloud Parameters and OLR

Cloud parameters are retrieved, and OLR is computed, for each FOV. The cloud parameter retrieval converges about 99% of the time. Cloud parameters and OLR are flagged as having best quality (QC=0) as long as the cloud parameter retrieval converges. Cloud parameters and OLR are flagged as QC=2 for those cases in which the cloud parameter retrieval does not converge, as are all other geophysical parameters.

3.5 The Fundamental Level-3 Test Used for Most Other Geophysical Parameters

The QC flags for $T(p)$, $q(p)$, T_s, cloud parameters, and OLR have already been discussed. Level-3 products for these geophysical parameters include all cases with QC=0 or QC=1. Level-3 products for all other geophysical parameters also include all cases with QC=0 or QC=1, but the QC flags for those geophysical parameters are defined in a different manner. At a minimum, all other geophysical parameters must pass the fundamental Level-3 test. In order to pass the fundamental Level-3 test, *PBest* or *PGood* must be equal to p_{surf}, that is, the entire temperature profile must be flagged as having at least good quality. The fundamental Level-3 QC test is used in the generation of QC flags used for T_s and ε_ν over land, and also for $CO(p)$, $CH_4(p)$, OLR_{CLR}, and the surface air temperature T_{sa}. If this test is not passed, the QC flag for these parameters is set equal to 2 and those cases are not included in the generation of those Level-3 parameters. The fundamental level-3 test is also referred to as the constituent test because it is used to generate QC flags for constituent profiles. The most obvious use of the fundamental Level-3 test for QC purposes is for T_{sa}, the surface air temperature, in which QC is set equal to 0 if *PBest* equals p_{surf}. QC is set equal to 1 if *PGood*, but not *PBest*, is equal to p_{surf}. QC is set equal to 2 otherwise. The same test is used to generate the QC flags for total precipitable water W_{tot}, and OLR_{CLR}.

The constituent test is not applied to ozone profiles, however since ozone is primarily in the upper atmosphere. Therefore accurate temperature retrievals near the surface are relatively unimportant, but accurate surface characterization matters. For this reason we do not apply the fundamental Level-3 test to O_3. For O_3 we include different checks for QC purposes. The first test is used to eliminate spurious cases in which dust contaminates the O_3 retrieval. Sand contains silicates, which absorb IR radiation in the ozone absorption

band near 1000 cm^{-1}. Absorption by sand results in spuriously high values of retrieved O_3 in these regions if not accounted for. The CHART and AIRS Version-7 retrieval algorithm attempt to reject such cases. The QC procedures reject O_3 in these areas using the dust tests developed by Sergio DeSouza-Machado (2006) and also rejects cases where the retrieved emissivity in the ozone spectral region differs from the first guess emissivity mode more than in adjacent spectral regions. Cases are also rejected where the converged state does not match the radiances sufficiently well. In addition, O_3 retrievals are rejected when the first iteration tries to make too large a change to total O_3. This situation is indicative of a problem elsewhere in the retrieval.

3.6 Error estimates and Quality Control for Clear Column Radiances $\hat{R}_i$

The error estimate and QC methodologies for the clear column radiances $\hat{R}_i$ are explained in detail in the AIRS Version-6 ATBD. The following section gives a brief overview of the use of error estimates for $\hat{R}_i$, $\delta\hat{R}_i$, and their use for QC purposes.

Different channels are sensitive, by varying amounts, to clouds at different pressures. Therefore, $\delta\hat{R}_i$ is both channel and case dependent. The retrieval output provides separate case dependent QC flag for each channel, based on thresholds of the case dependent values of $\delta\hat{R}_i$. Even if significant cloud clearing errors exist for some channels in a given case, channels that have little or no sensitivity to the clouds in that case would have very accurate values of $\hat{R}_i$. It is for this reason that we assign each channel its own case dependent QC flags indicating whether the cloud-cleared radiance $\hat{R}_i$ is of sufficient accuracy for use for different purposes. Clear column radiances in channels with QC=0 for a given retrieval case are considered to have the highest accuracy, and are recommended for potential use in data assimilation experiments. Clear column radiances in channels with QC=1 are considered to be of good quality and are recommended for inclusion in other applications, such as process studies. Clear column radiances in channels with QC=2 are not recommended for scientific use. The methodology used to generate $\delta\hat{R}_i$ was designed to accommodate the assimilation of $\hat{R}_i$ as a part of a data assimilation scheme. The QC procedure is based on $\delta\hat{\theta}_i$, where $\delta\hat{\theta}_i$ is the channel brightness temperature error estimate given by $\delta\hat{\theta}_i = \widehat{\delta R}_i \left(\frac{dB}{dT}\right)^{-1}_{\hat{\theta}_i}$ and $\hat{\theta}_i$ is the clear column brightness temperature for channel i. $\hat{R}_i$ is flagged as highest quality (QC=0) if $\delta\hat{\theta}_i \leq$ 1K, and $\hat{R}_i$ is flagged as good quality (QC=1) if $\delta\hat{\theta}_i$ is greater than 1.0 K, but less than or equal to 2.5 K.

4. Single Day Comparison of Quality Controlled CrIS and AIRS Retrievals

Agreement between CrIS CHART and AIRS Version-7 retrievals is a requirement toward the CrIS CHART serving as an adequate follow on to AIRS Version-7 from the climate monitoring perspective. In this and subsequent sections, CrIS CHART results are referred to as CrIS, and AIRS Version-7 results are referred to as AIRS. In this section, Quality Controlled CrIS and AIRS retrievals are shown and compared for the single day of April 15, 2016. Two types of results are shown: 1) single day statistical comparisons, and 2) single day Level-3 spatial plots. Single day statistical comparisons are important because they indicate relative acceptance rates and accuracies of QC'd CrIS and AIRS retrievals for the same day. Single day Level-3 spatial plots are important because they compare spatial coverages, differences, and accuracies of CrIS and AIRS retrievals. In the Level-3 comparison, it should be borne in mind that CrIS and AIRS spatial coverages are not exactly the same, nor are the satellite zenith angles in which a scene is observed by each instrument. CrIS swath widths are wider than those of AIRS because the SNPP orbit, on which CrIS flies, is at a higher altitude than that of Aqua, on which AIRS flies.

4.1 *T(p)* and *q(p)* retrieval accuracy as a function of yield

Figure 2 shows statistics of the differences of QC'd CrIS and AIRS retrievals from collocated ECMWF truth for a sample day. Panel (a) shows the percentage of QC'd cases accepted as a function of height, panel (b) shows RMS differences of 1 km layer mean temperatures from collocated ECMWF "truth", and panel (c) shows biases of QC'd 1 km layer mean differences from ECMWF. Statistics are shown for two sets of QC thresholds, those passing the highest standard (*PBest*), which we suggest for use for Data Assimilation purposes, and those passing good QC, which are used for the creation of Level-3 products used for climate research. We show in red the results for CrIS retrievals and in black results for AIRS retrievals using analogous QC procedures. The two black horizontal lines are at 500 mb and 700 mb.

The *T(p)* and *q(p)* QC methodology does not apply any test which eliminates the entire temperature profile, other than the requirement that the retrieval runs to completion. Retrievals using the tighter DA thresholds have lower yields, and smaller errors, with RMS errors on the order of 1 K. Retrievals with this accuracy have been found to be optimal for use for data assimilation purposes. CrIS retrievals at 500 mb with DA thresholds are accepted 60% of the time. This allows for the assimilation of CrIS temperature products above the clouds, even in storms as well as in overcast conditions.

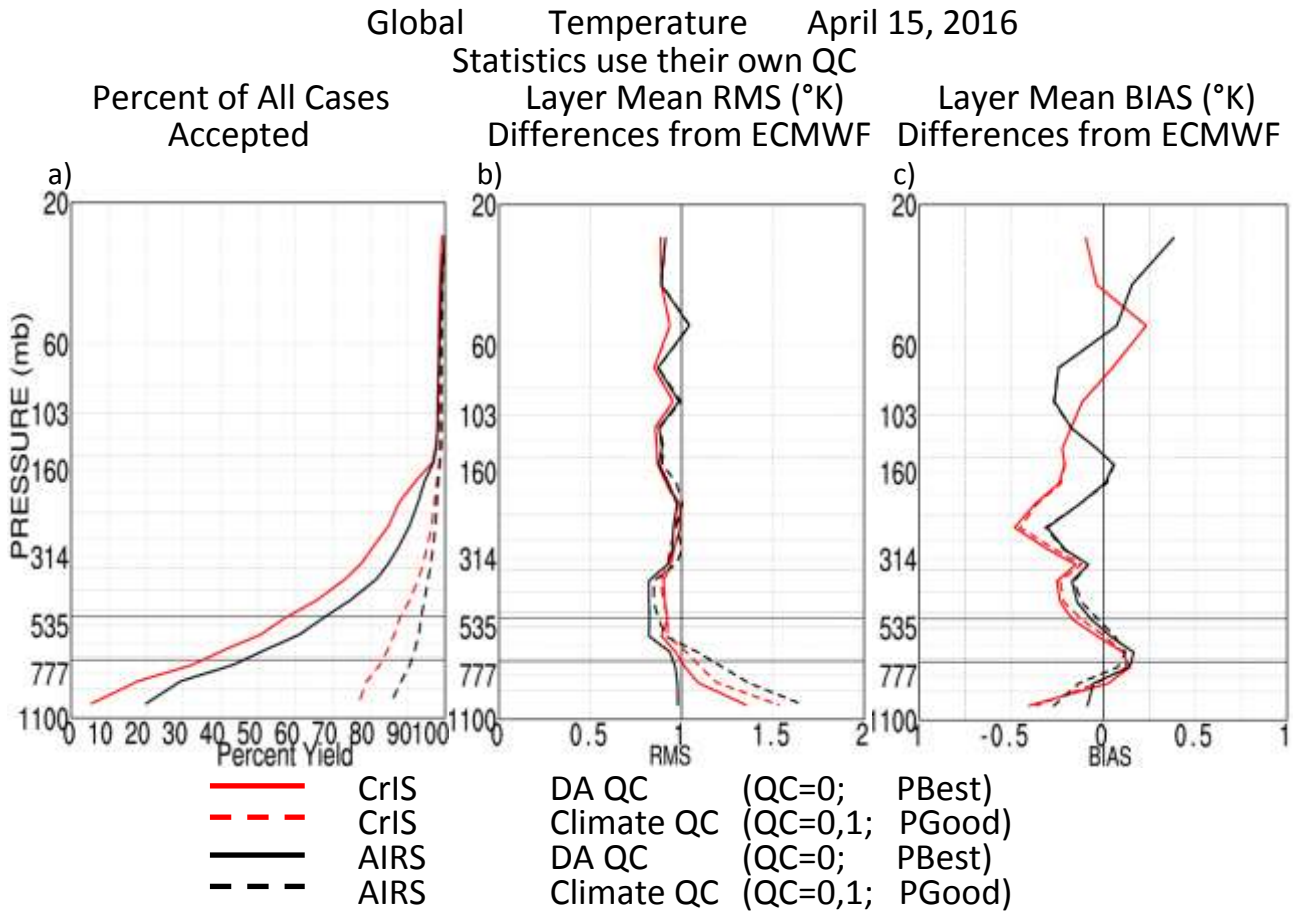

Figure 2

The yields of CrIS and AIRS retrievals with Climate QC are both extremely high throughout the atmosphere, with values at the surface of about 75% for CrIS and 85% for AIRS. Achievement of this very high yield is extremely valuable in the generation of highly representative Level-3 Climate Data sets, which should have at best only a minimal amount of clear sky bias.

Figure 3 compares CrIS and AIRS Level-3 500 mb temperatures with each other for the ascending (1:30 PM) and descending (1:30 AM) local time orbits for April 15, 2016. Grid boxes containing no data are shown in gray. This situation occurs between orbit gaps and in other places where data is missing. It also occurs in grid boxes where all retrievals are rejected. CrIS observations have a wider swath than do AIRS, and therefore the CrIS orbit gaps are narrower than those of AIRS. Agreement between CrIS and AIRS 500 mb temperature is extremely good, with global mean biases less than 0.1 K, and spatial correlations of 1.00. The differences between CrIS and AIRS 1:30 PM 500 mb temperatures poleward of 70°N both sides of the dateline are the result of mismatches in

time between the CrIS and AIRS observations included in the Level-3 product. This artifact does not occur in the 1:30 AM Level-3 products shown.

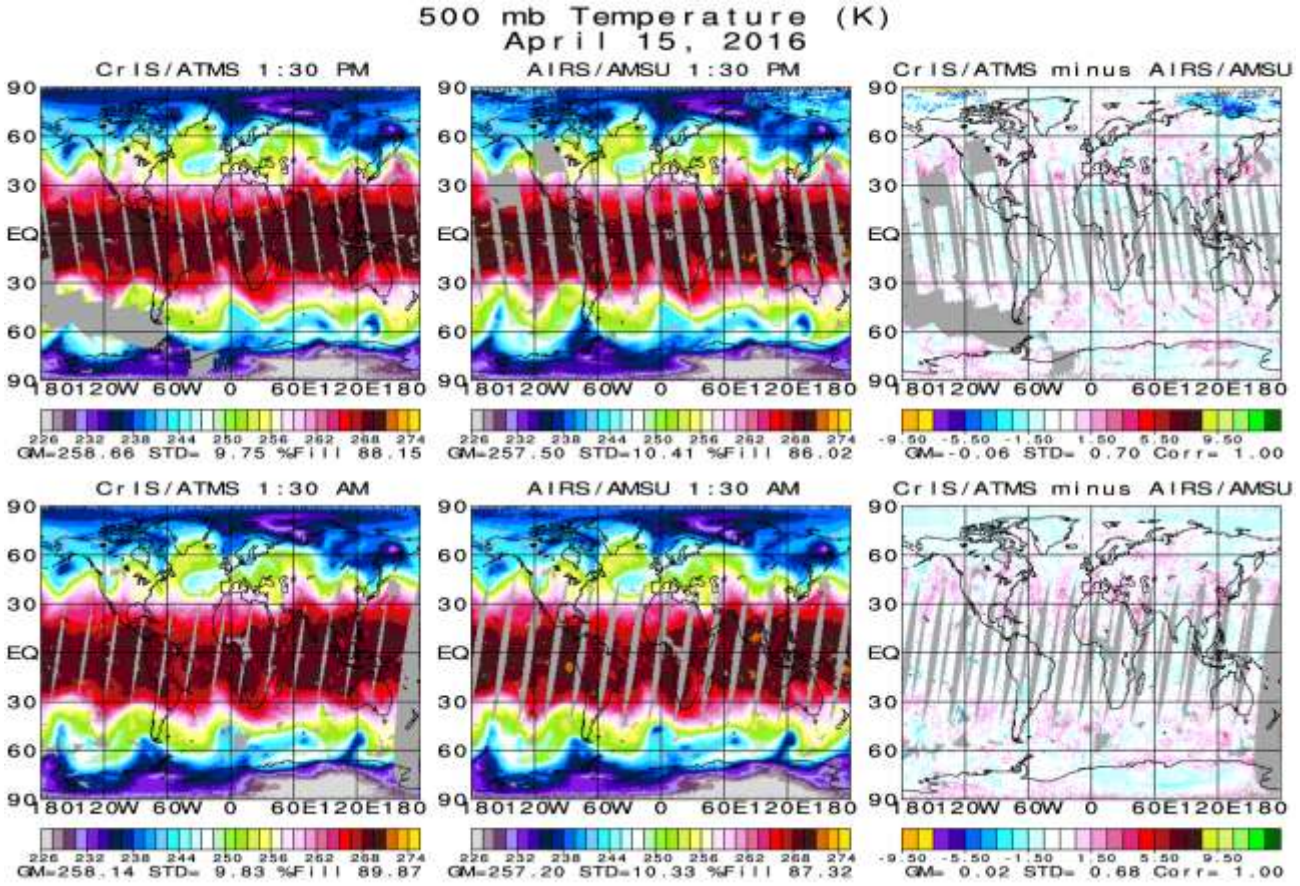

Figure 3

Figure 4 shows analogous results to those of Figure 2, comparing QC'd 1 km layer precipitable water to that of collocated values of ECMWF. We show results only up to 200 mb, above which water vapor retrievals are considered to be of minimal validity. As with regard to *T(p)*, the yield for accepted CrIS *q(p)* retrievals with either set of QC threshold is somewhat lower than that of AIRS. Unlike AIRS, CrIS *q(p)* retrievals are unbiased compared to ECMWF, and, like AIRS, have high accuracy.

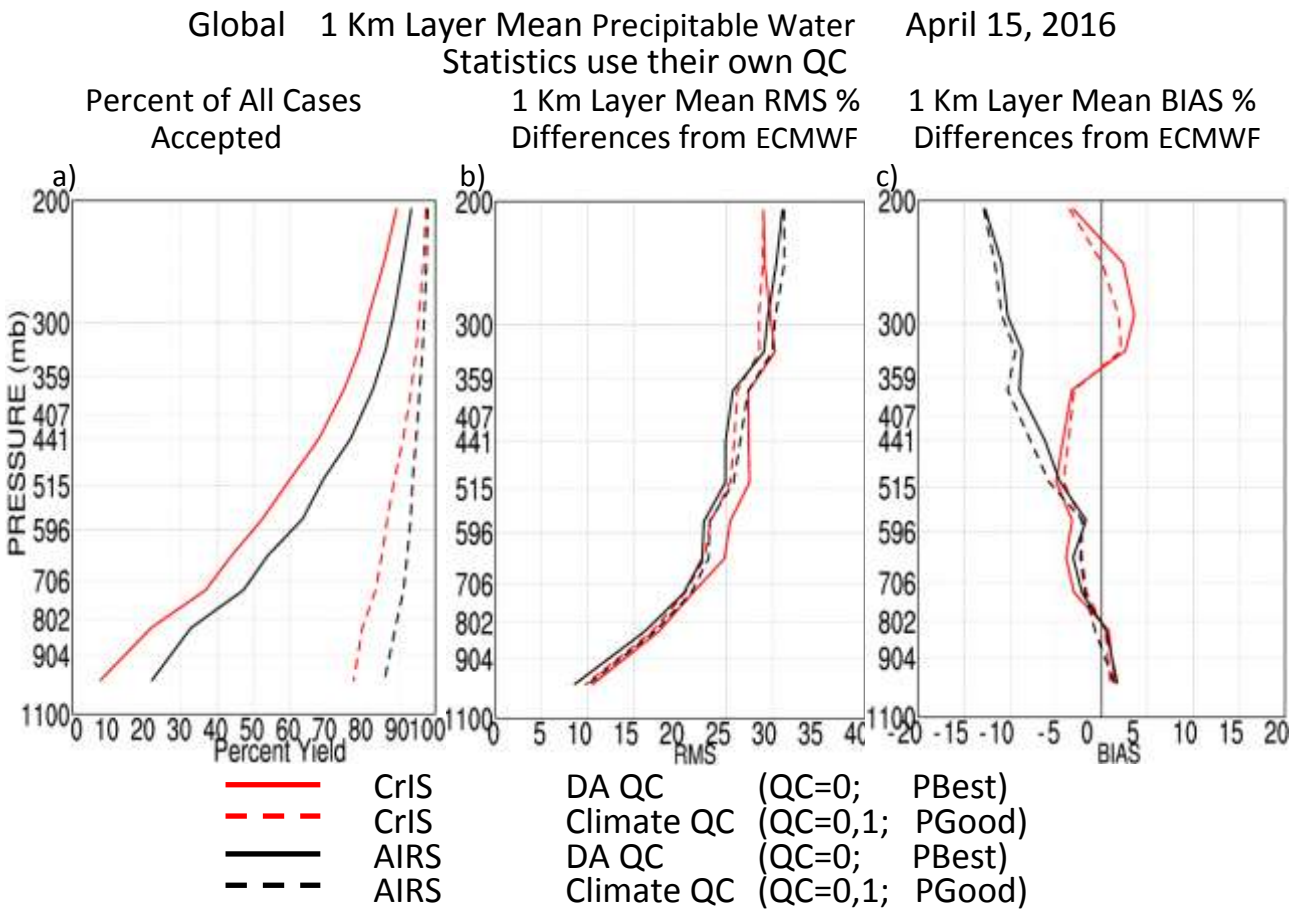

Figure 4

Figure 5 compares CrIS and AIRS Level-3 total precipitable water with each other for the ascending and descending 1:30 local time orbits for April 15, 2016. Total precipitable water is accepted if the constituent test is passed. This requires that *PBest* or *PGood* be equal to the surface pressure, p_{surf}. AIRS and CrIS single day Level-3 total precipitable water fields agree extremely well with each other, in terms of both biases as well as spatial standard deviations and correlations.

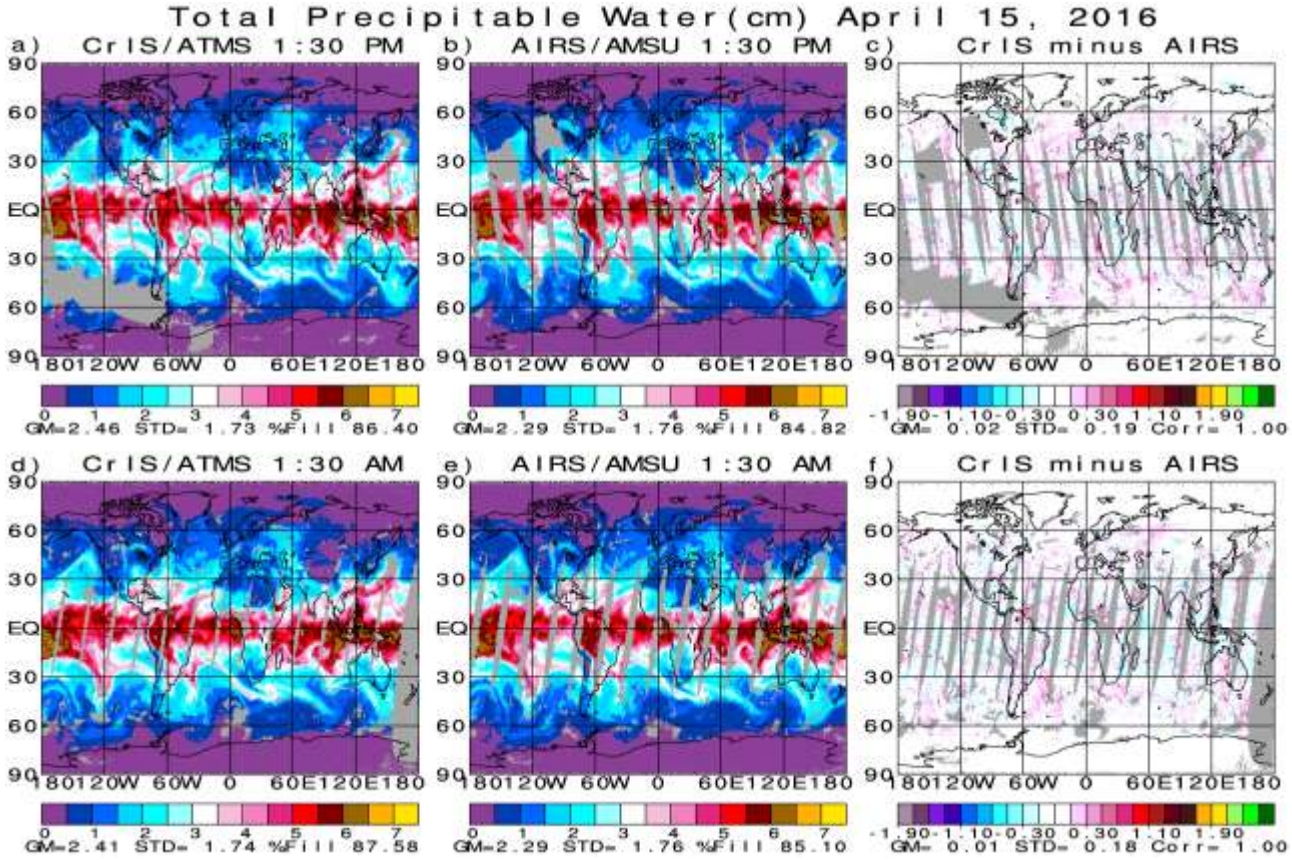

Figure 5

4.2 Ocean Surface Skin Temperature T_s and Surface Spectral Emissivity ε_ν

The term T_s refers to surface skin temperature over all surfaces. We also refer to values of T_s over non-frozen ocean as Sea Surface Temperature (SST). Figure 6 shows counts of Quality Controlled SSTs, over the latitude range, 50˚N – 50˚S, as a function of the difference between T_s and ECMWF "truth". ECMWF "truth" for T_s, and for most other geophysical parameters, is taken from the ECMWF 3-hour forecast field. We show the counts of CrIS retrievals in red and pink, and of AIRS retrievals in black and gray. The lighter shade of each color shows counts of best quality T_s retrievals, obtained using tight error estimate thresholds (QC=0). The darker shade shows counts of both best and good quality T_s retrievals, including cases with QC=0 or 1, where the error estimate thresholds for QC=1 are looser than those for QC=0. Ocean T_s retrievals with QC=0 or 1 are the ensemble used to generate the Level-3 SST product used for climate studies.

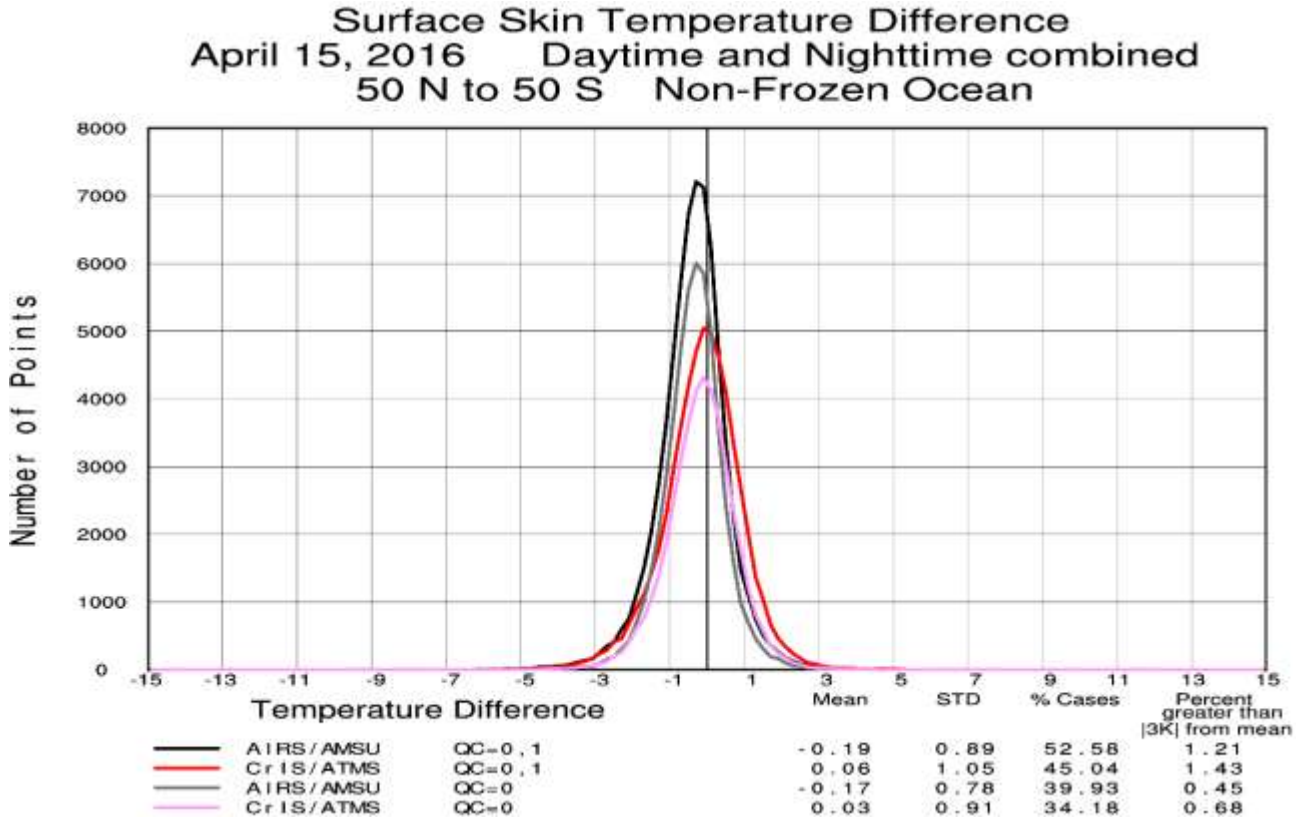

Figure 6

Figure 6 contains statistics for each set of retrievals showing the mean difference from ECMWF, the standard deviation of the ensemble differences, the percentage of all possible cases included in the Quality Controlled ensemble, and percentage of all accepted cases with absolute differences from ECMWF of more than 3K from the mean difference. Such cases are referred to as outliers. CrIS QC'd SST retrievals accept somewhat fewer cases than AIRS and contain somewhat higher standard deviations of the errors. This might be the result of the fact that the CrIS shortwave window, from which T_s is determined, does not extend as far as that of AIRS. In both ensembles, the percentage of outliers grows with loosening the QC thresholds as expected.

Figure 7 shows the spatial distribution of the differences of the Level-3 oceanic SST between 50°N and 50°S from collocated ECMWF values for both CrIS and AIRS. The values shown in a given grid box are the average values for that grid box of all cases in which the SST retrieval was accepted. Oceanic cases shown in gray indicate grid boxes in which there were orbit gaps or missing data due to the QC procedure. The CrIS Level-3 SST product is slightly poorer compared to ECMWF than that of AIRS in terms of spatial STD.

Ocean Surface Skin Temperature (K) 50°N to 50° S April 15, 2016

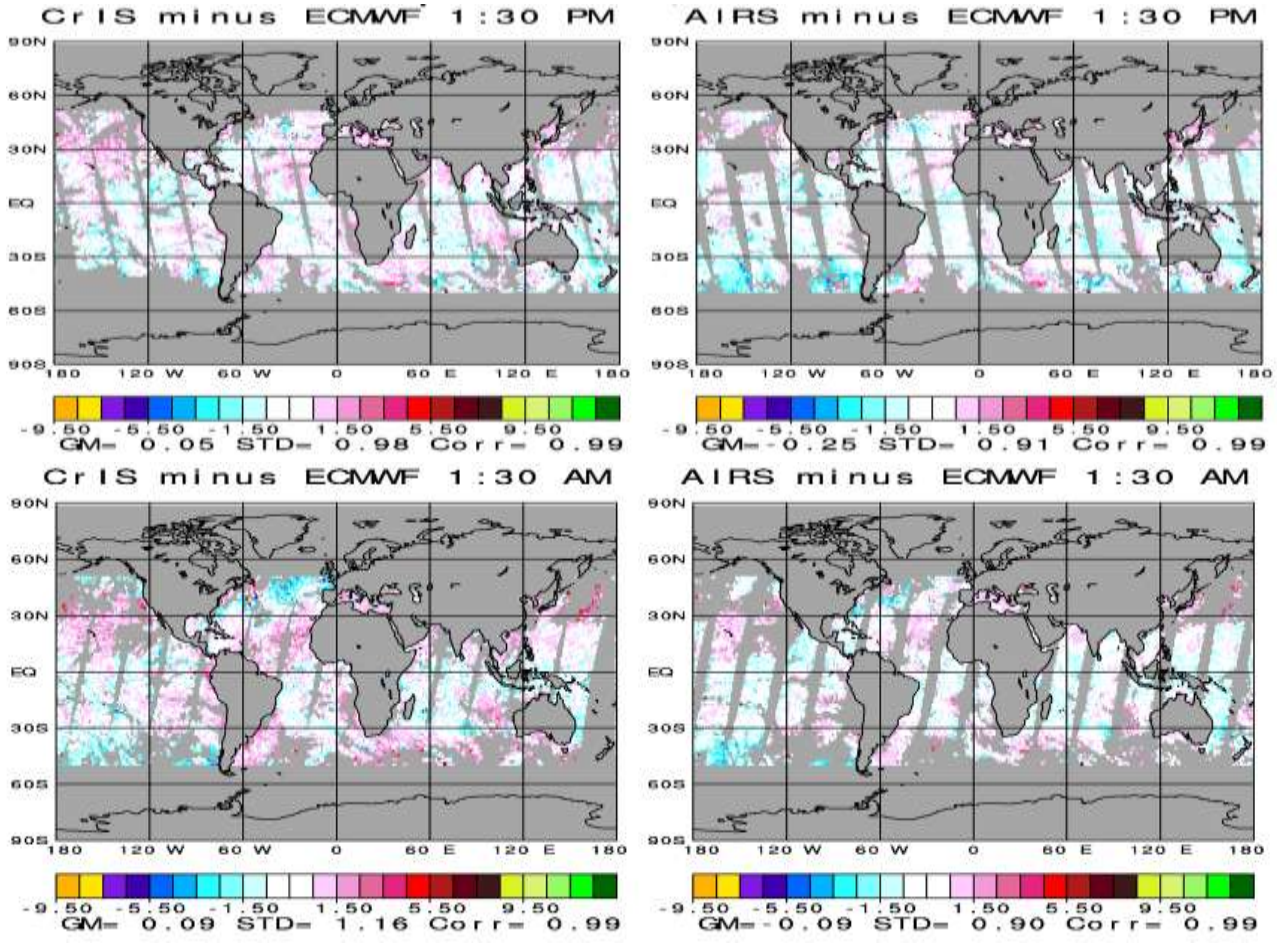

Figure 7

Figures 8a and 8b show the mean difference of the retrieved ocean surface emissivity ε_ν from that of the Masuda AIRS Science Team ocean surface emissivity model. Results are shown as a function of satellite zenith angle for ν = 950 cm^{-1}, and ν = 2400 cm^{-1}, respectively. Figures 8c and 8d show the standard deviations of the retrieved values at a given zenith angle for both AIRS and CrIS. The two channels shown are in the longwave and shortwave window regions respectively. In these figures, statistics are shown separately for AM orbits in dark colors, and PM orbits in light colors. Figures 8a and 8b show that daytime and nighttime retrieved values of AIRS ocean surface emissivity in both spectral regions are very close to each other and are also in very good agreement with the ocean emissivity model, Masuda, which is a good measure of truth. CrIS PM and AM ocean emissivities are in poorer agreement with Masuda, as well as with each other, in both spectral regions. The degradation of CrIS retrievals shows up in both the mean and

standard deviation senses. CrIS ocean surface emissivity results appear to be poorer at night than during the day in terms of agreement with AIRS results and Masuda.

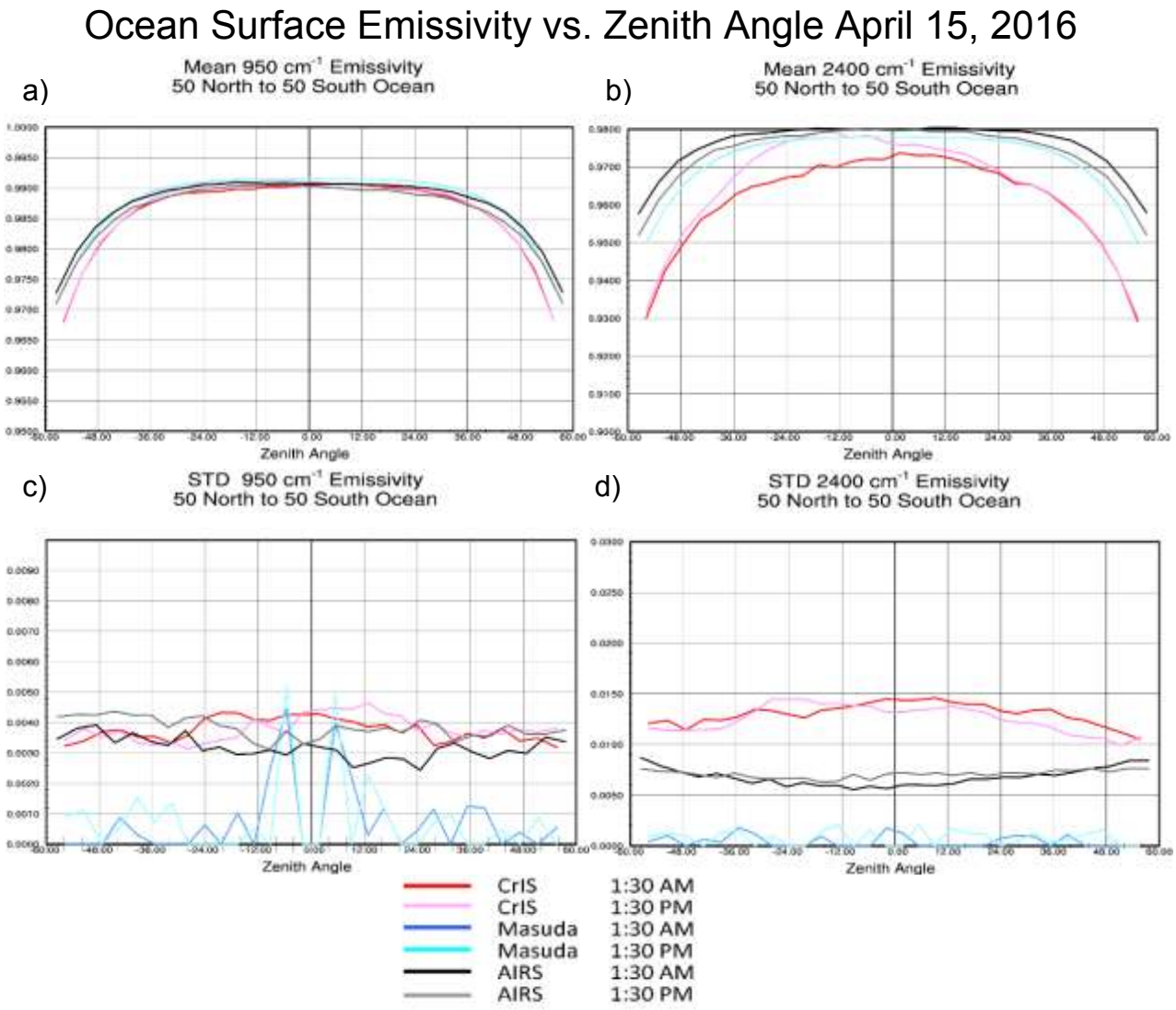

Figure 8

4.3 Land Surface Temperature and Spectral Emissivity

Figure 9 compares CrIS and AIRS surface skin temperature over both land and ocean for the ascending and descending orbits of April 15, 2016. Agreement between CrIS and AIRS SST values are extremely good. CrIS LST values agree somewhat less well with AIRS, especially in polar areas in both Hemispheres, where LST is very cold. In these areas, CrIS LST is warmer than that of AIRS and may well not be cold enough.

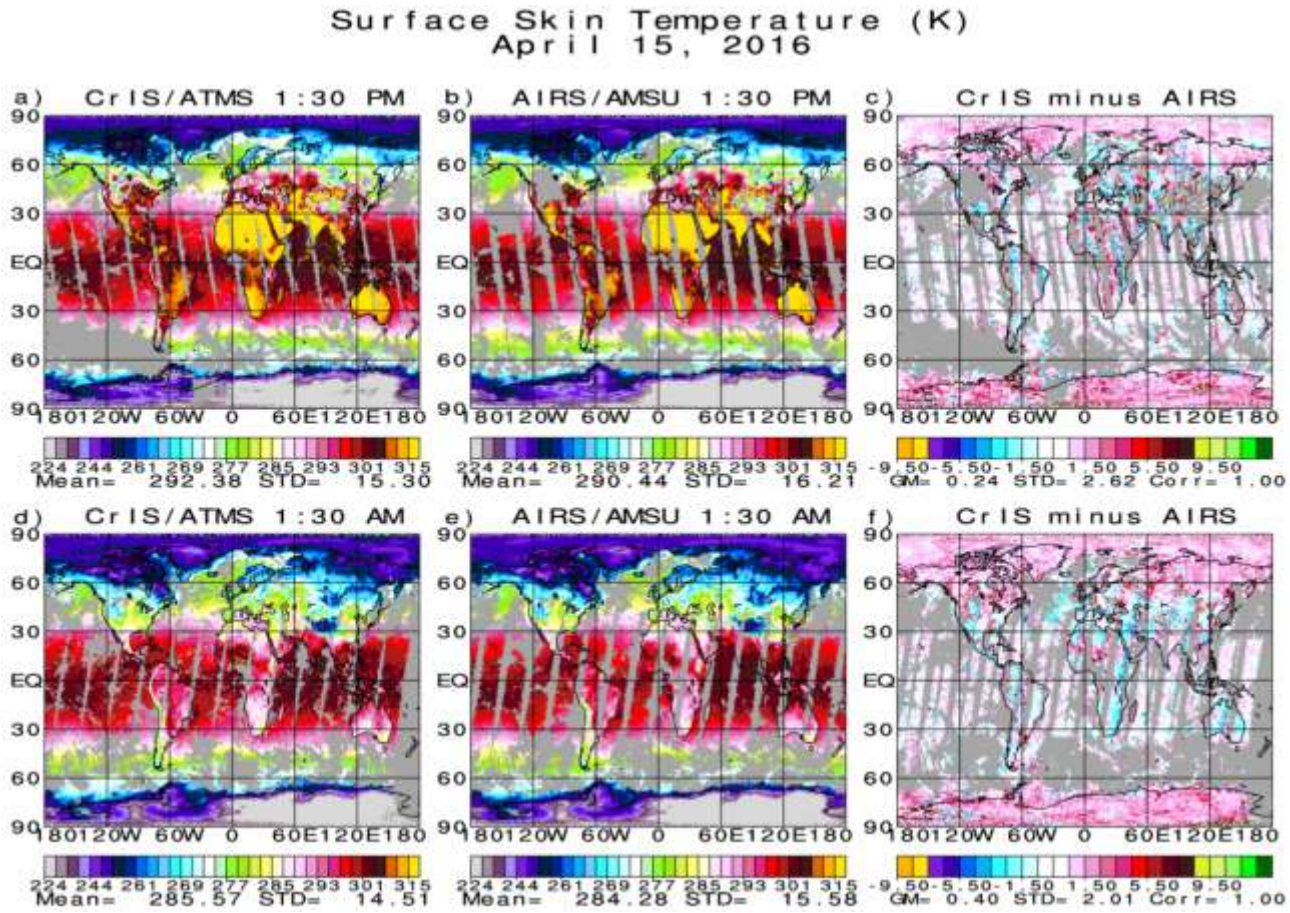

Figure 9

Figure 10 shows differences over land of 1:30 PM retrieved values of ε_ν from those at 1:30 AM, at 950 cm^{-1} and 2400 cm^{-1}. Over land, surface spectral emissivity values change rapidly in space and season as a result of differences in ground cover. At a given location and day, these values should not change appreciably from day to night, however. Day/night land surface emissivity differences are very small for AIRS in both spectral regions, but are much larger for CrIS, especially at 2400 cm^{-1}. The degradation in both CrIS ocean emissivities (Figure 8) and land surface emissivities (Figure 10) compared to those of AIRS is most likely a consequence of CrIS having less SW spectral coverage than AIRS, on the one hand, and how we treat that factor in the retrieval process on the other hand. More research is needed here to possibly further improve the CrIS surface skin temperature and surface spectral emissivity retrieval methodologies.

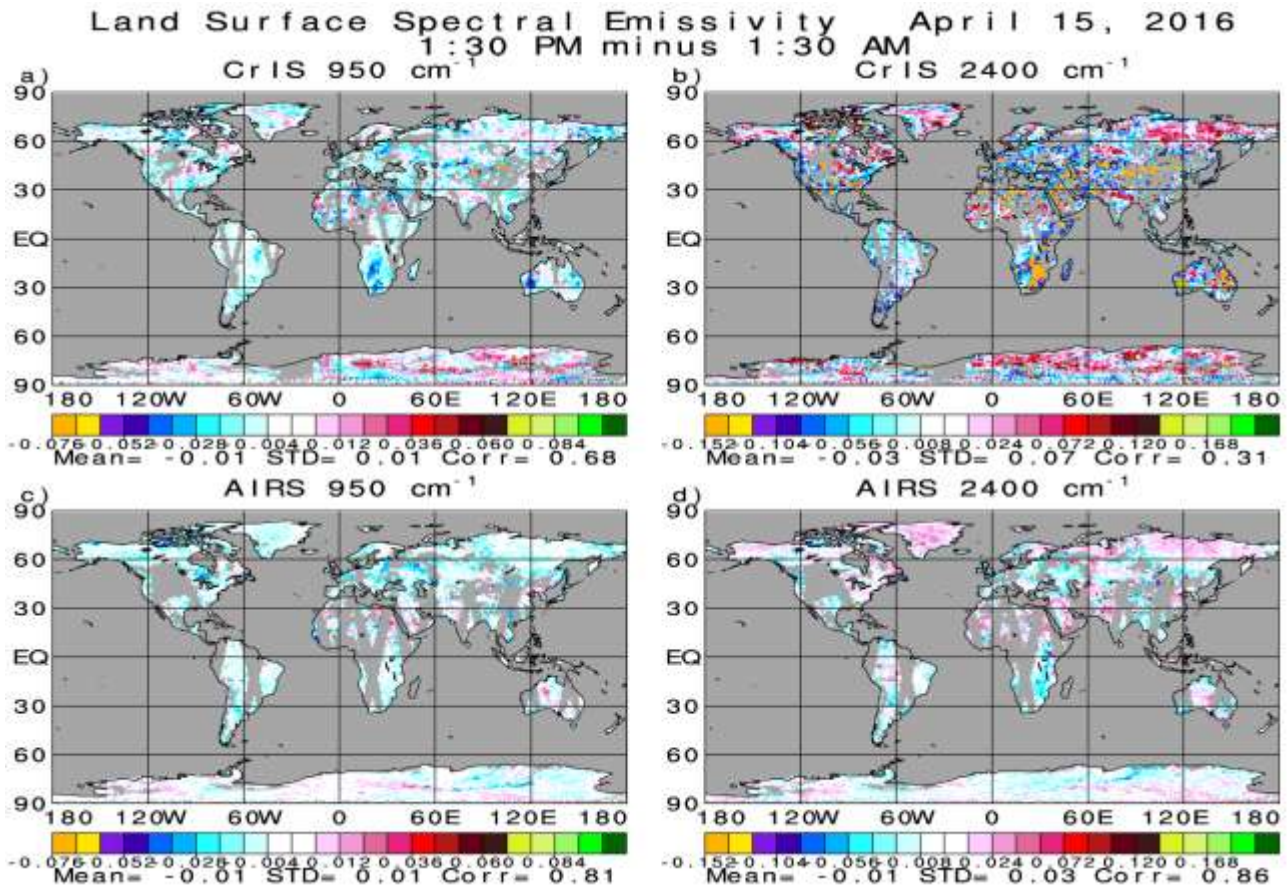

Figure 10

4.4 Retrieval of Cloud Fraction $\alpha\varepsilon$ and Cloud Top Pressure p_c

The radiatively effective cloud fraction at frequency ν, $\alpha\varepsilon_\nu$, is given by the product of the geometric fractional cloud cover of a FOV as seen from above, α, and the cloud spectral emissivity ε_ν. The cloud parameter retrieval methodology determines only the product of these two terms, $\alpha\varepsilon_\nu$, and a corresponding cloud top pressure p_c, for each of up to two layers of clouds in a given scene as seen from above (Susskind et al., 2003). A basic assumption of the cloud retrieval methodology is that the clouds are gray, i.e., $\alpha\varepsilon_\nu$ is independent of frequency. Susskind et al. (2003) simultaneously derived nine pairs of effective cloud fractions $\alpha\varepsilon_1$ and $\alpha\varepsilon_2$, one pair for each FOV ℓ contained within the ATMS (CrIS/ATMS) or AMSU (AIRS/AMSU) FOR, along with two cloud top pressures p_{c1}, and p_{c2} representative of the pressures of each of the two layers of clouds covering the entire FOR. Subsequent versions of the retrieval system algorithms solve for separate cloud top pressures in each FOV. The cloud parameter retrieval step is performed separately for

each FOV ℓ to determine nine pairs of $\alpha\varepsilon_{1\ell}$, $\alpha\varepsilon_{2\ell}$, $p_{c1\ell}$, and $p_{c2\ell}$. In addition, a total radiatively effective cloud fraction for the entire FOR, $\alpha\varepsilon$, is computed according to

$$\alpha\varepsilon = \sum_{\ell=1}^{9}\left(\alpha\varepsilon_{1,\ell} + \alpha\varepsilon_{2,\ell}\right)/9 \quad (4)$$

and an effective cloud top pressure for the entire FOR is computed as the weighted average of all 18 values of *pc* in the FOR.

$$p_c = \sum_{\ell=1}^{9}\left(\alpha\varepsilon_{1,\ell}\ p_{c1,\ell} + \alpha\varepsilon_{2,\ell}\, p_{c2,\ell}\right)/\sum_{\ell=1}^{9}\left(\alpha\varepsilon_{1,\ell}\ + \alpha\varepsilon_{2,\ell}\right). \quad (5)$$

The Level-2 product contains values of $\alpha\varepsilon_{1\ell}$, $\alpha\varepsilon_{2\ell}$, $p_{c1\ell}$, and $p_{c2\ell}$ for each FOV, as well as the single FOR heritage values $\alpha\varepsilon$ and p_c defined according to Equations 4 and 5.

A complication in the cloud parameter retrieval methodology is that the best least squares fit may result from a cloud parameter solution which lies in a region which is unphysical. In particular, we do not allow retrieved cloud fractions to be less than zero or greater than 100%, nor do we allow cloud pressures to be very close to the surface or above the tropopause.

Figure 11 shows the spatial distributions of values of cloud fraction $\alpha\varepsilon$ and cloud top pressure p_c for the daytime and nighttime orbits on April 15, 2016 as retrieved using the CrIS and AIRS data. Essentially all cloud parameter retrievals are accepted with the exception of the 1% of the time in which the cloud parameter retrieval fails to converge. These plots depict both $\alpha\varepsilon$ and p_c at the same time. There are seven different color scales used for different intervals of p_c, as indicated on the figures. Reds, violets and purples indicate high clouds, blues and greens indicate mid-level clouds, and oranges and yellows indicate low clouds. Within each color scale, darker colors indicate larger fractional cloud cover, and paler colors indicate lower fractional cloud cover. Cloud fractions are indicated by a given shade with cloud fractions grouped in five intervals: 0-20%, 20-40%, 40-60%, 60-80%, and 80-100%. Retrieved AIRS and CrIS cloud fractions and cloud top pressures match each other extremely well. They should not be expected to match perfectly on a given day because AIRS and CrIS see a given location at slightly different times, and also at different zenith angles. Cloud fractions observed at larger zenith angles tend to be larger than those at low zenith angles because more sides of clouds are observed. Spatial coverages of both CrIS and AIRS cloud parameters are both slightly higher than those of 500 mb temperatures because no other QC procedure is applied to cloud parameters other than the cloud parameter retrieval convergence.

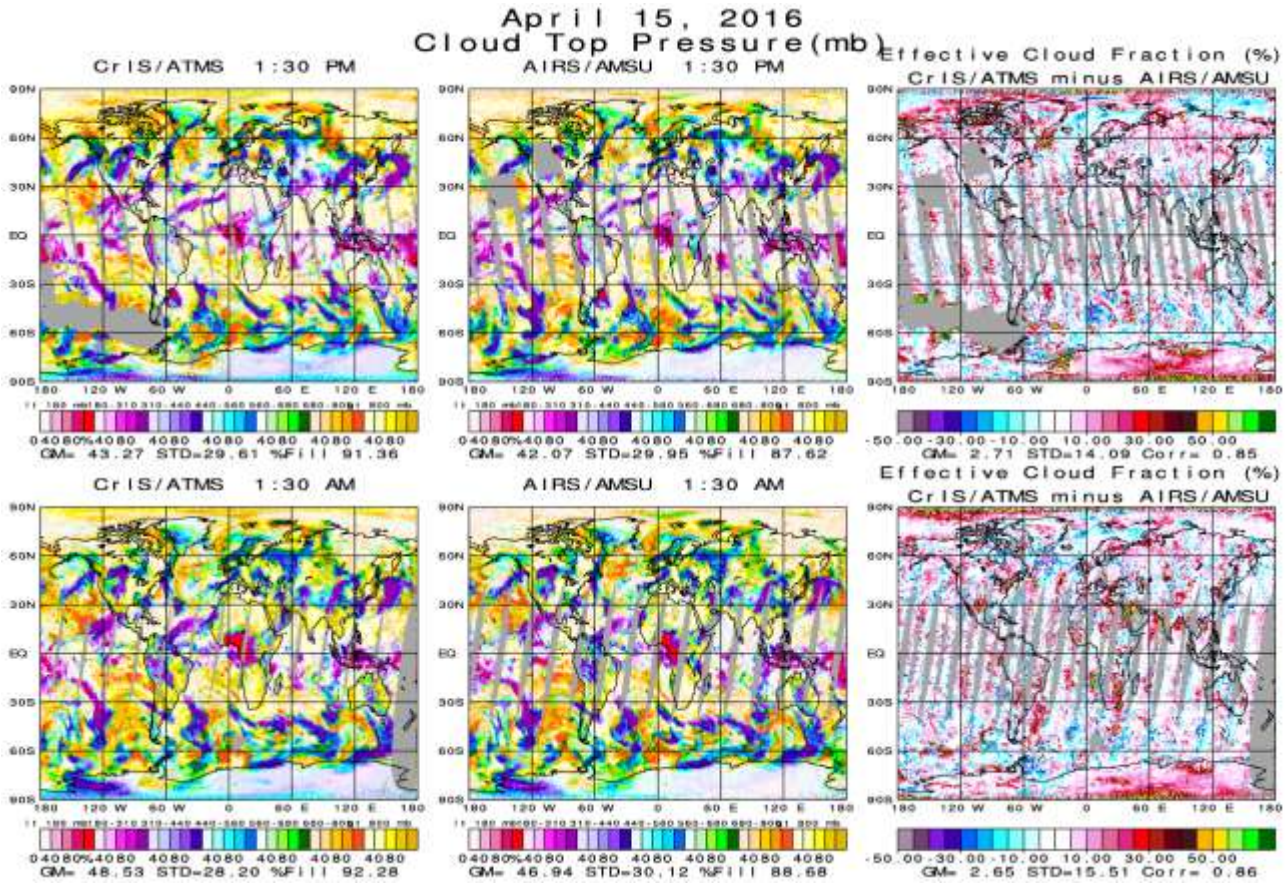

Figure 11

4.5 OLR and Clear Sky OLR (OLR_{CLR})

4.5.1 OLR

OLR at a given location is affected primarily by the earth's skin surface temperature, T_s; skin surface spectral emissivity, ε_ν; atmospheric vertical temperature profile, $T(p)$; and water vapor profile, $q(p)$; as well as the heights, amounts, and spectral emissivities of multiple layers of cloud cover. OLR also depends on the vertical distributions of trace gases such as $O_3(p)$, $CH_4(p)$, $CO_2(p)$, and $CO(p)$. Susskind et al. (2012) describes the OLR RTA used to compute OLR and OLR_{CLR} in AIRS Version-6, and which is the same as that used in Version-7. CHART and AIRS OLR is computed on a FOV basis. OLR is accepted if the cloud parameter retrieval has converged. OLR therefore has the same spatial coverage as the cloud fields shown in Figure 11.

Figure 12 compares Level-3 CrIS and AIRS OLR products obtained for the ascending (1:30 PM) orbits and descending (1:30 AM) orbits for April 15, 2016. Global mean CrIS and AIRS

OLR values agree with each other to better than 2 W/m^2. Agreement is better at 1:30 AM than 1:30 PM, where there appears to be some differences in the times at which CrIS and AIRS are sampled as discussed previously.

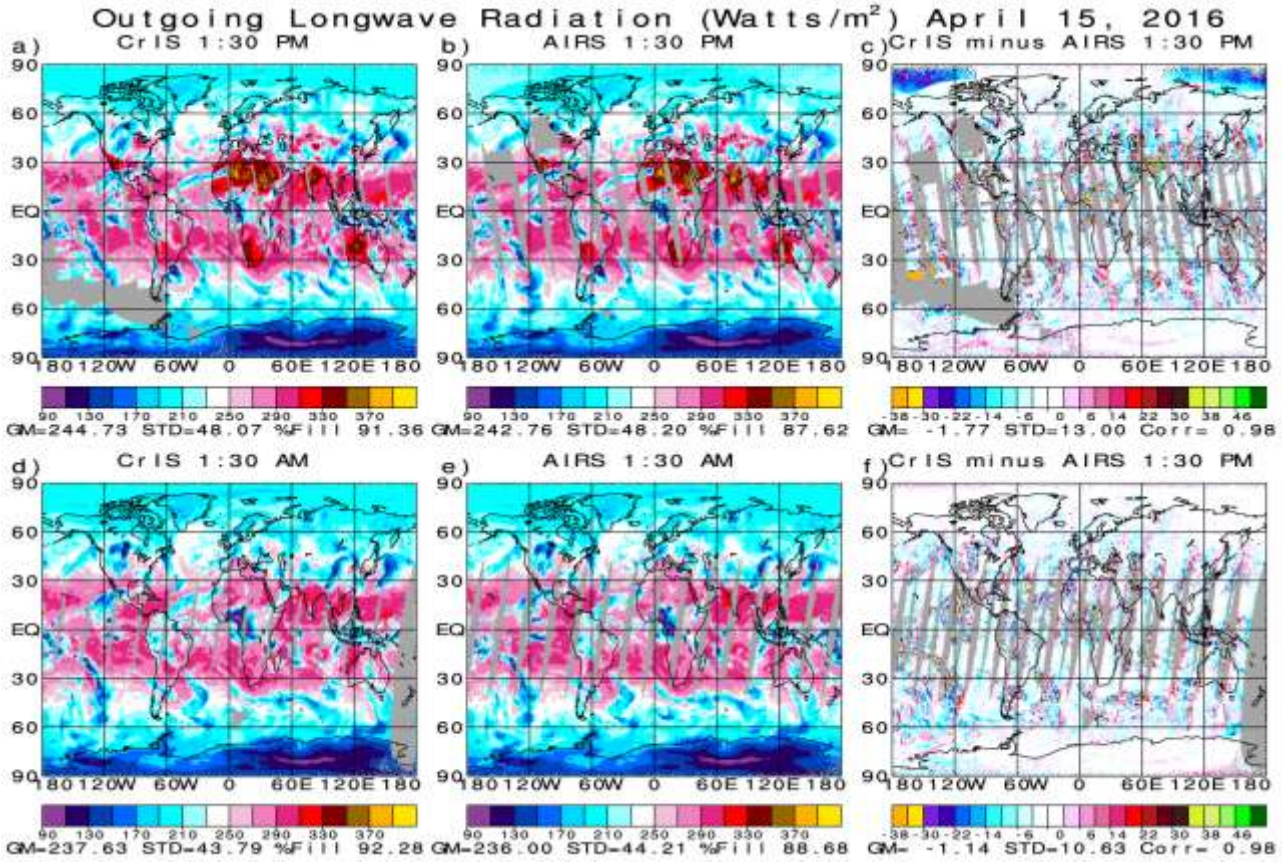

Figure 12

4.5.2 OLR_{CLR}

The OLR_{CLR} product is designed to represent the longwave flux going to space emanating from the clear portion of a FOV as observed under partial cloud cover conditions. Values of OLR_{CLR} are included in the Level-3 product only for those FOVs which pass the constituent test. This occurs if the retrieved surface air temperature is flagged as having good or best quality. Figure 13 is analogous to Figure 12, but for values of CrIS and AIRS OLR_{CLR}. The spatial coverages of CrIS and AIRS values of OLR_{CLR} are both lower than the corresponding values for OLR because values of OLR_{CLR} have to pass the constituent test to be accepted. The spatial coverage of OLR_{CLR} is therefore the same as that of total precipitable water. The agreement between CrIS and AIRS values of OLR_{CLR} is extremely good in terms of both global mean and spatial standard deviation.

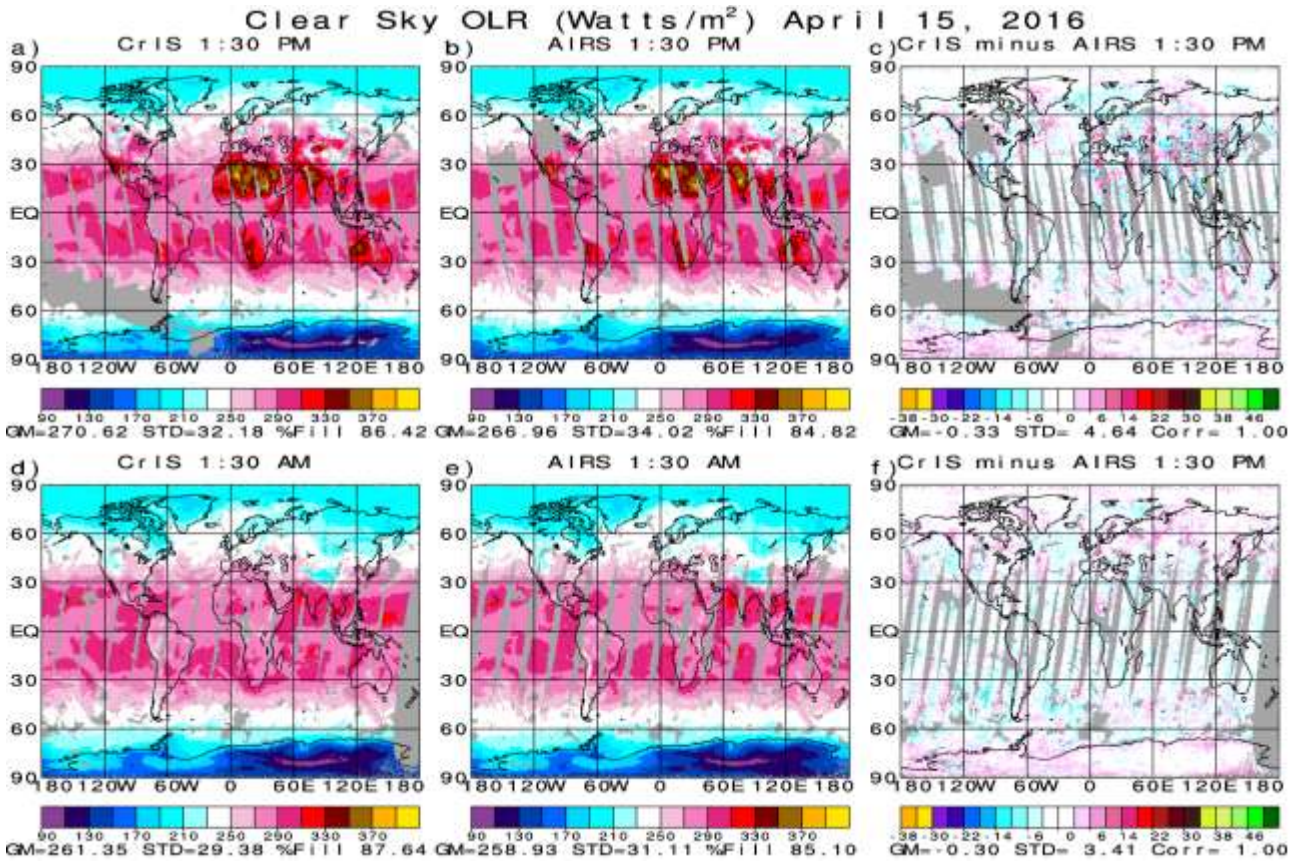

Figure 13

4.6 Total Ozone

Figure 14 compares Level-3 CrIS and AIRS total ozone for the ascending and descending orbits of April 15, 2016. CrIS and AIRS Level-3 total ozone products agree extremely well with each other in terms of both bias and spatial standard deviation. The spatial coverage of CrIS and AIRS Level-3 total ozone is somewhat lower than that of clouds or OLR because of the use of tests that flag dusty cases as of poor quality. Note for example the spatial gaps over the Sahara desert and off its west coast.

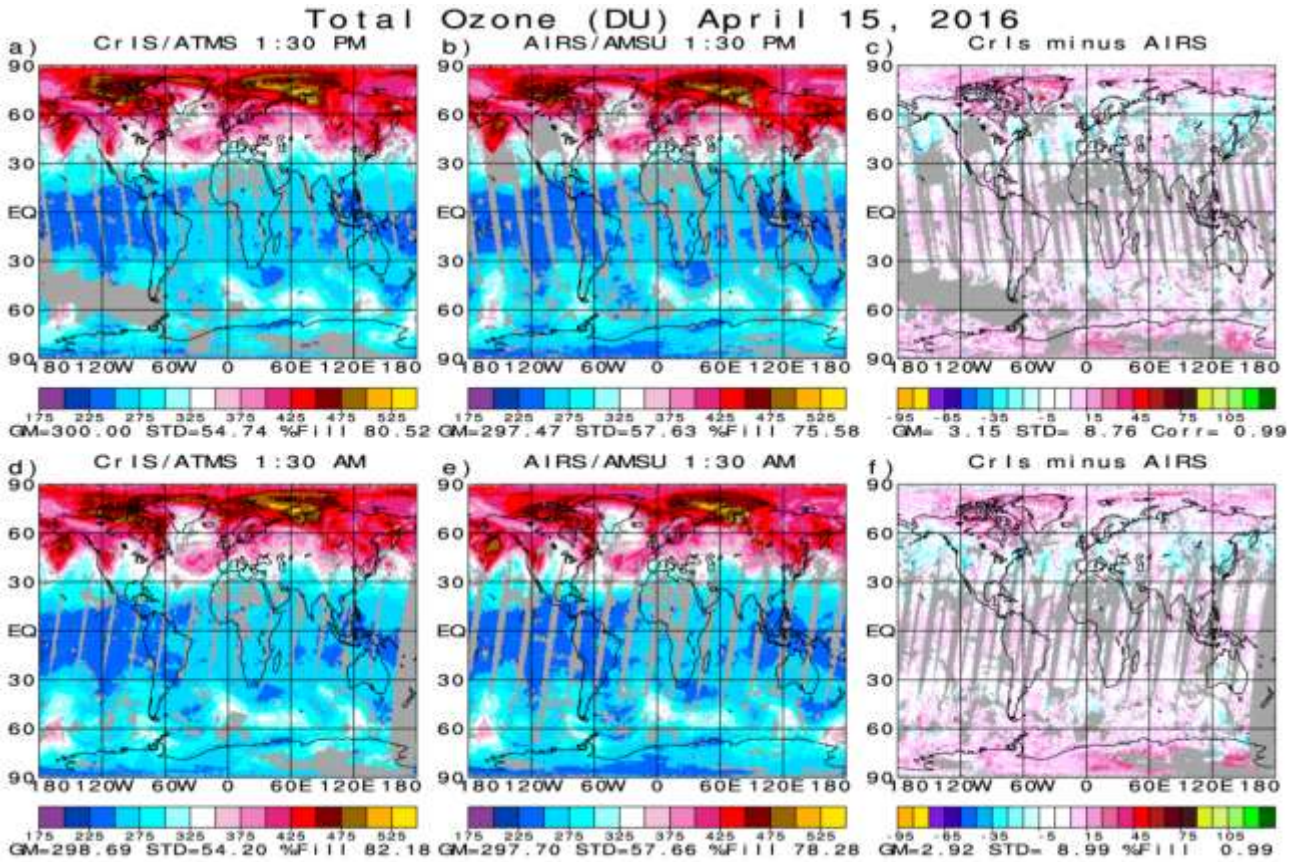

Figure 14

4.7 Clear Column Radiances

Figure 15 displays spectral characteristics of CrIS clear column radiances with Quality Flags QC=0, and also with QC=0 or 1, over the entire spectral domain. The results shown are for all global cases that were observed by CrIS over the single day under study. All results are shown in the brightness temperature domain.

The top panel in Figure 15 shows the mean clear column brightness temperature spectrum of all cases with QC=0 and 1. The brightness temperature for a given channel corresponds to a weighted average temperature over the pressure interval to which the channel radiance is sensitive. Higher brightness temperatures occur in channels primarily sensitive to mid-lower tropospheric temperatures as well as in windows, which are sensitive primarily to surface skin temperatures. The longwave window lies between 800 cm^{-1} and 1000 cm^{-1}, and the shortwave window covers the spectral range 2400 cm^{-1} to 2550 cm^{-1}. Channels at frequencies centered on absorption lines sense higher in the atmosphere than those off the corresponding lines, and therefore have lower brightness temperatures when sensing the

troposphere, and higher brightness temperatures when sensing the stratosphere. The transition between the two domains occurs at roughly 710 cm^{-1}.

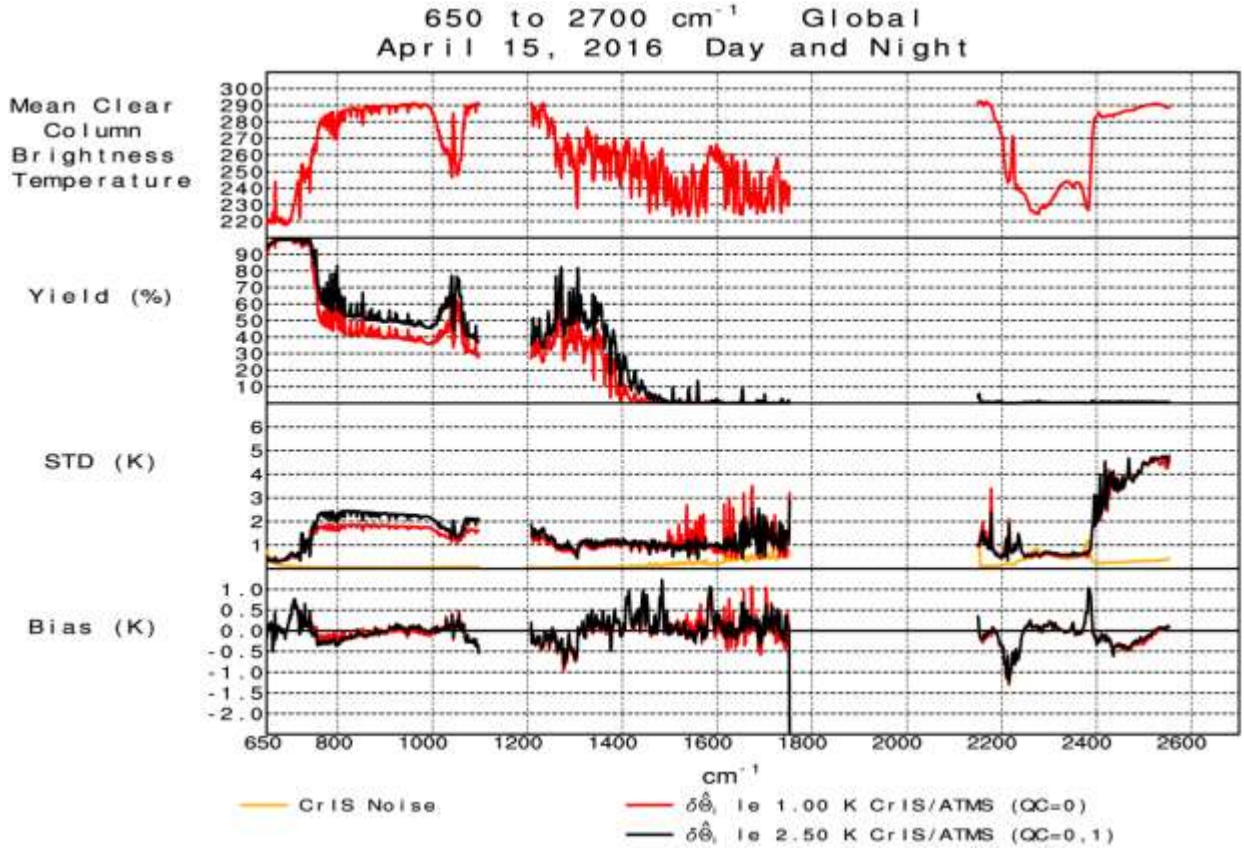

Figure 15

The second panel of Figure 15 shows the percentage of all FOR's in which $\hat{\theta}_i$ was found acceptable using each of the 1.0K and 2.5K criteria for $\delta\hat{\theta}_i$. Yields increase at frequencies lower than 710 cm^{-1}, in which channels are primarily sensitive to radiation emitted higher in the atmosphere, and hence are less sensitive to clouds in the field of view. For the same reason, yields are higher at frequencies located on absorption lines than those located off those lines. Therefore yields are higher at frequencies with local minima of brightness temperatures when sensing the troposphere, and are higher at frequencies with local brightness temperature maxima when sensing the stratosphere. Yields with QC=0,1 are higher than those with QC=0, especially as the channels become more sensitive to mid-lower tropospheric temperatures. Yields of accepted cloud cleared radiances in the water vapor absorption band, between 1400 cm^{-1} and 1750 cm^{-1}, are all near zero because our current method relies on the ECMWF water vapor used to compute Θ_i^{truth}.

The third panel in Figure 15 shows the standard deviations (STD) of the quality-controlled values of $\left(\hat{\Theta}_i - \Theta_i^{truth}\right)$. The yellow line shows the mean value of the single spot channel noise $NE\Delta T_i$ when evaluated at 250 K. Actual noise in $\hat{\Theta}_i$ can be less than its channel $NE\Delta T$ for stratospheric channels, because the radiances observed over the nine FOV's in the FOR can be averaged to obtain $\hat{R}_i$, as these channels are for the most part unaffected by clouds. The standard deviations of the errors in $\hat{\Theta}_i$ are larger using cases with QC=0,1, compared to QC=0, especially for channels more sensitive to lower tropospheric and surface skin temperatures. The increases in the standard deviation of the errors in $\hat{\Theta}_i$ for lower tropospheric sounding channels is partly a result of larger cloud effects on the radiances for those channels (errors in $\hat{\Theta}_i$), and partly the result of a larger contribution of the surface used in the computation of Θ_i^{truth} (errors in Θ_i^{truth}), because ECMWF has significant skin temperature errors over land.

The lowest panel of Figure 15 shows the bias of the differences between $\hat{\Theta}_i$ and Θ_i^{truth}. Part of these biases result from errors in the computation of Θ_i^{truth} as a result of both radiative transfer errors, as well as errors in X^{truth}. For example, the positive biases, on the order of 0.5K, between $\hat{\Theta}_i$ and Θ_i^{truth} found for channels sounding the stratosphere are certainty not a result of cloud clearing errors. Rather they are the result of errors in the ECMWF stratospheric temperatures used to compute Θ_i^{truth}.

5. Comparison of CrIS/ATMS and AIRS Monthly Mean Products

The main objective of the CrIS/ATMS CHART retrieval system is to generate monthly mean Level-3 products which are compatible with those of AIRS Version-7, so as to make CrIS/ATMS Climate Data Records provide a seamless follow-on to those of AIRS. Prototype Version-7 retrievals for the month of July 2015 have been processed by the AIRS Science Team for AIRS and by the JPL Sounder SIPS for CrIS/ATMS. This section shows two sets of comparisons: 1) comparison of CrIS/ATMS and AIRS/AMSU July 2015 monthly mean products with each other to demonstrate their compatibility; and 2) comparisons of select CrIS and AIRS monthly mean products with analogous monthly mean products derived from other highly regarded data sources, so as to both compare CrIS and AIRS products with each other, and also to validate each set of products.

5.1 Comparison of Select CrIS and AIRS Monthly Mean Products with Each Other

Figure 16 compares CrIS and AIRS July 2015 mean fields of surface skin temperature and total precipitable water with each other. These fields agree very well with each other. Monthly mean CrIS surface skin temperatures are slightly warmer than those of AIRS over Antarctica, where the earth's surface is extremely cold, and CrIS skin temperatures might

not be cold enough. This potential shortcoming in CrIS surface skin temperatures in very cold areas was also apparent in Figure 9.

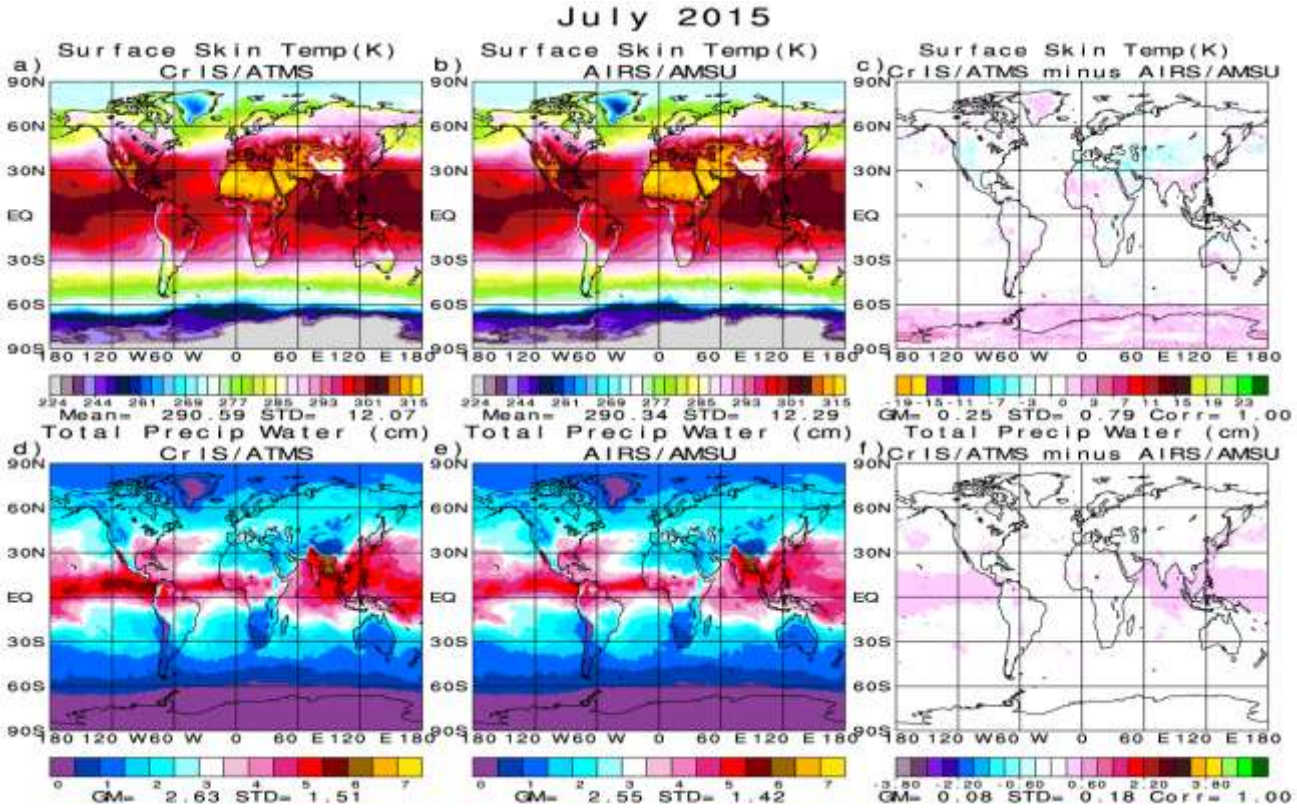

Figure 16

CrIS and AIRS monthly mean fields of total precipitable water also agree extremely well with each other. CrIS monthly mean total precipitable water for July 2015 is slightly higher than that of AIRS over tropical ocean in areas containing very large amounts of total precipitable water. CrIS is probably more accurate than AIRS in these oceanic areas because it has the benefit of ATMS, which provides very accurate total precipitable water over ocean.

Figure 17 compares CrIS and AIRS monthly mean 500 mb temperatures and 300 mb temperatures with each other for July 2015. CrIS and AIRS agreement is almost perfect in both fields, both with regard to global means as well as spatial standard deviations.

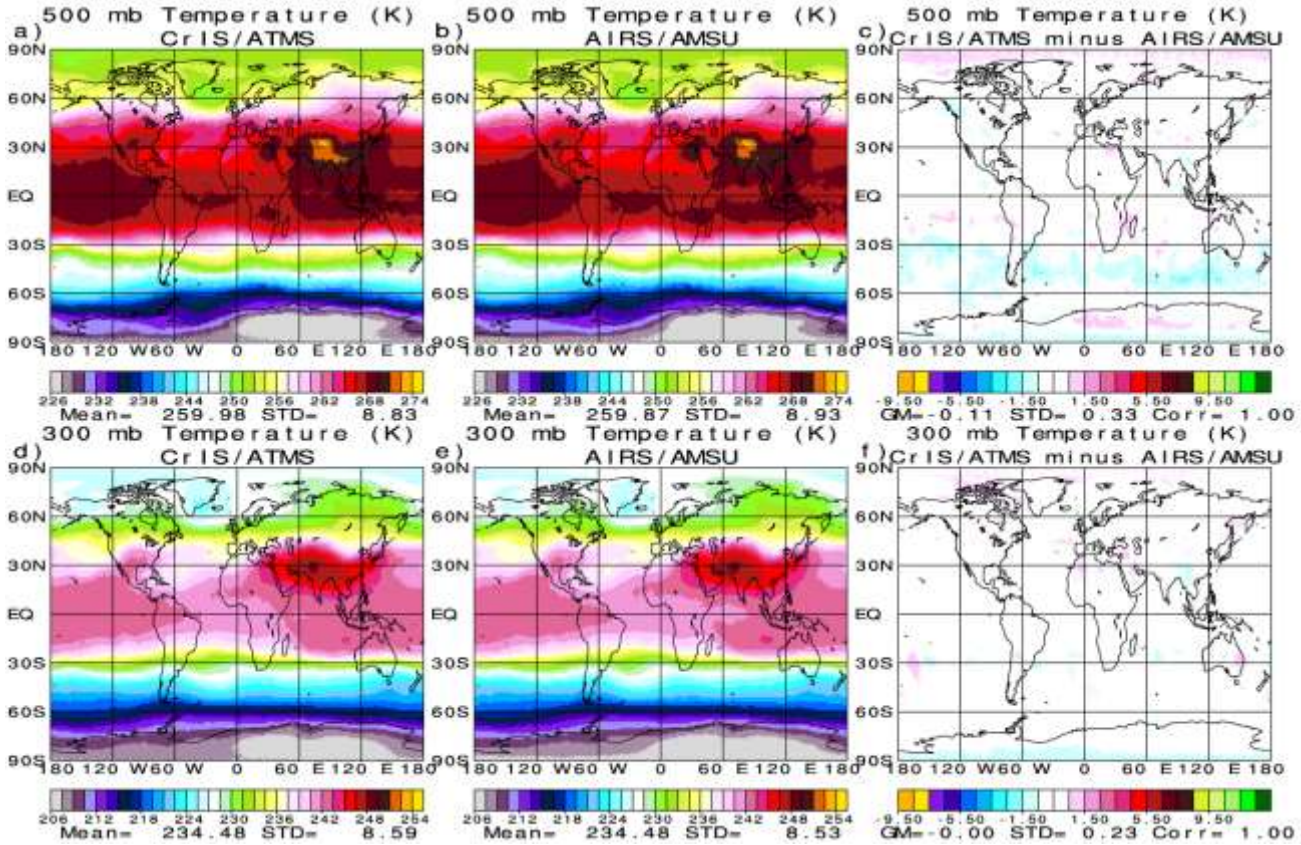

Figure 17

Figure 18 compares CrIS and AIRS monthly mean cloud parameters and clear sky OLR products with each other for July 2015. The agreement between CrIS and AIRS cloud products, and also between CrIS and AIRS clear sky OLR is both extremely good. The largest differences occur over Antarctica, where CrIS surface skin temperatures are warmer, and probably less accurate, than those of AIRS. CrIS generates more cloud cover than AIRS over Antarctica because CrIS skin temperatures in this area are probably spuriously too warm, and therefore more clouds are retrieved so as to generate computed radiances which are consistent with the observed radiances in those channels used to determine the cloud parameters.

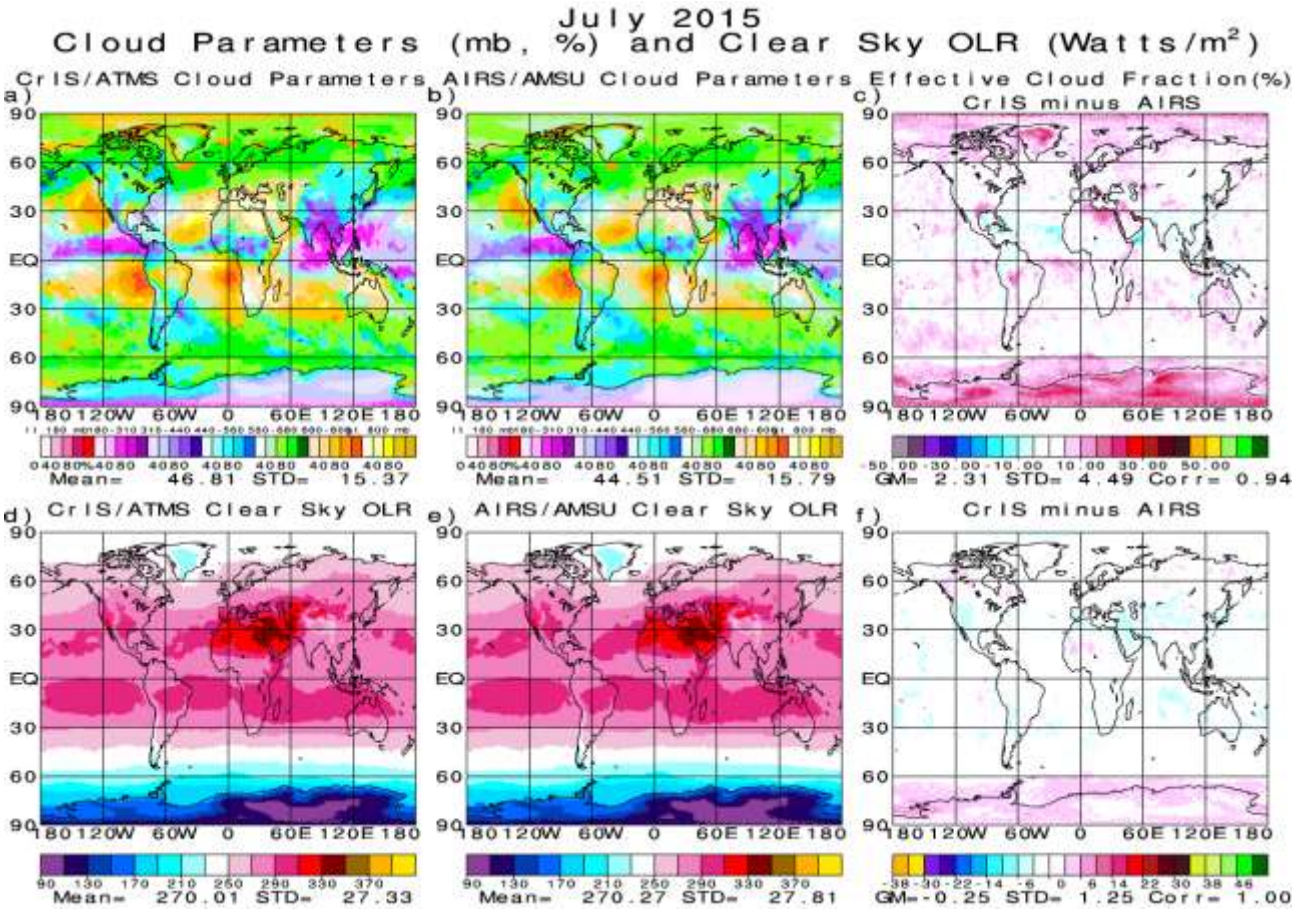

Figure 18

5.2 Comparison of Select CrIS and AIRS Monthly Mean Products with those of Other Measures of the same Geophysical Parameters

5.2.1 OLR

Figure 19 compares CrIS and AIRS July 2015 monthly mean values of OLR with each other and with CERES Edition-4.0. CERES is considered the gold standard of OLR.

CrIS and AIRS July monthly mean values of OLR agree extremely well with each other and both agree very well with those of CERES. The largest differences between CrIS and AIRS OLR from those of CERES occur over land in areas containing large diurnal cycles of surface skin temperature. This phenomenon is explained in Susskind et al. (2018a, 2018b). These papers show that AIRS Version-6 OLR, as well as anomalies of AIRS Version-6 OLR, both agree extremely well with those of CERES over the period September 2002 through 2016. Agreement of July 2015 CrIS OLR with CERES is even better than that of AIRS.

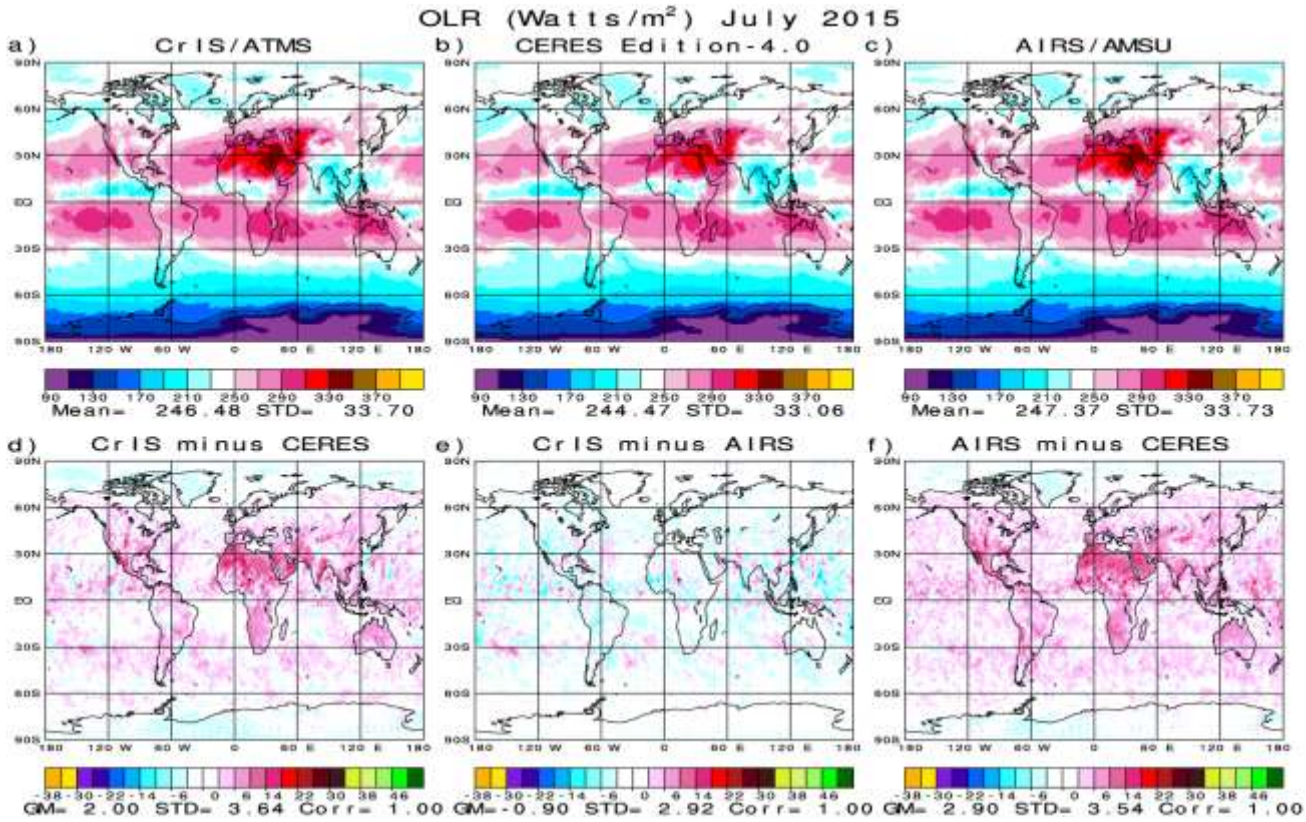

Figure 19

5.2.2 Total ozone

Figure 20 compares CrIS and AIRS total ozone fields with each other, and also with that of Ozone Mapping and Profiling Suite (OMPS). OMPS is considered the gold standard of total ozone. OMPS has no data poleward of 60°S in July 2015, because it is a UV instrument that requires sunlight. CrIS and AIRS total ozone fields agree extremely well with each other and also with that of OMPS in areas where OMPS contains data. CrIS July 2015 total ozone actually agrees better with OMPS, in terms of spatial standard deviation, than does AIRS, which is already extremely good.

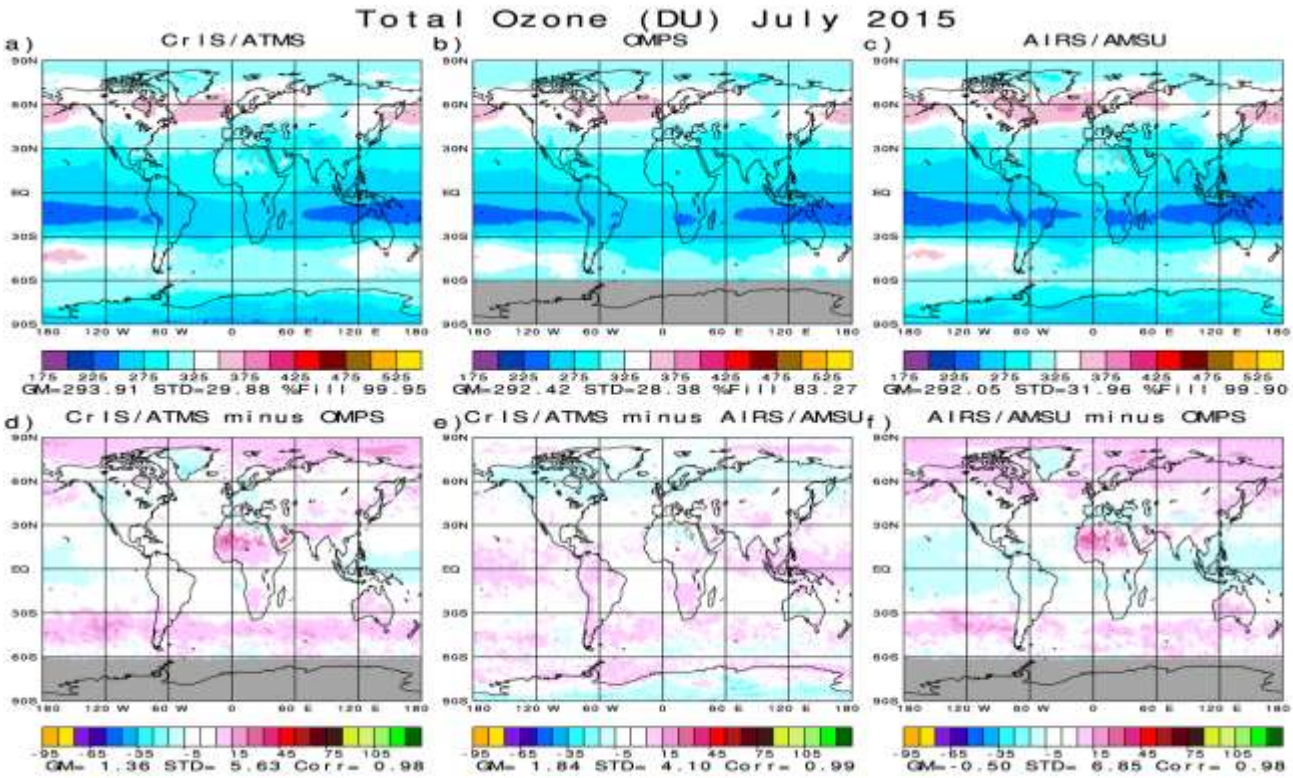

Figure 20

6. Implications toward meeting the goal of the research

The goal of the research is to generate CrIS/ATMS level-3 products, so as to provide a seamless transition from those of AIRS for the purpose of climate research. Figures 16 through 20 are very encouraging in terms of the excellent agreement of CrIS and AIRS products, and also show that some CrIS monthly mean products are at least as accurate as those of AIRS for the two products where AIRS has already been shown to be very accurate by comparison with “Gold Standard” products. The comparison shown in Figures 16 through 20 must also be done comparing CrIS and AIRS monthly mean products for months in different seasons, in which, hopefully, agreement between CrIS and AIRS monthly mean products will be as good. Even more important for data continuity of AIRS climate data records with those of CrIS is comparison of interannual differences of CrIS and AIRS monthly mean products. Global mean bias, or even local biases, between CrIS and AIRS monthly mean products become less significant if these biases are further reduced in the interannual difference sense.

REFERENCES

AIRS ATBD documentation https://eospso.gsfc.nasa.gov/atbd-category/37

Barnet, C., Blaisdell, J.M., and Susskind, J., "Practical methods for rapid and accurate computation of interferometric spectra for remote sensing applications," *IEEE Trans. Geosci. Remote Sens.*, vol. 38, no. 1, pp. 169–183, Jan. 2000.

Boylan, P., J. Wang, S. A. Cohn, E. Fetzer, E. S. Maddy, and S. Wong , Validation of AIRS version 6 temperature profiles and surface-based inversions over Antarctica using Concordiasi dropsonde data, J. Geophys. Res. Atmos., 120, 992–1007, doi:10.1002/2014JD022551, 2015.

DeSouza-Machado, S., L. L. Strow, S. E. Hannon, and H. E. Motteler, "Infrared dust spectral signatures from AIRS", Geophysical Research Letters, Vol. 33, L03801, doi:10.1029/2005GL024364, 2006.

Fetzer, E. J. (2006), Preface to special section: Validation of Atmospheric Infrared Sounder Observations, J. Geophys. Res., 111, D09S01, doi:10.1029/2005JD007020.

Gambacorta, A., "The NOAA Unique CrIS/ATMS Processing System (NUCAPS): Algorithm Theoretical Basis Documentation." *NOAA Center for Weather and Climate Prediction (NCWCP), Version* 1 (2013).

Lambrigtsen, B, Suomi National Polar Partnership Mission, NASA L1b: Advanced Technology Microwave Sounder, ATBD, Version 1, July 2014, JPL.

Milstein, A. B., and W. J. Blackwell (2016), Neural network temperature and moisture retrieval algorithm validation for AIRS/AMSU and CrIS/ATMS, J. Geophys. Res. Atmos., 121, 1414–1430, doi:10.1002/2015JD024008.

Nasiri, S.L., H. Van T. Dang, B.H. Kahn, E.J. Fetzer, E.M. Manning, M.M. Schreier, and R.A. Frey, 2011: Comparing MODIS and AIRS Infrared-Based Cloud Retrievals. *J. Appl. Meteor. Climatol.,* **50**, 1057–1072, https://doi.org/10.1175/2010JAMC2603.1

Seemann, S.W., E. E. Borbas, R. O. Knuteson, G. R. Stephenson, H.-L. Huang, 2007: Development of a Global Infrared Land Surface Emissivity Database for Application to Clear Sky Sounding Retrievals from Multi-spectral Satellite Radiance Measurements. J. of Appl. Meteor. and Climatol., Vol. 47, 108-123.

Susskind, J., Barnet, C.D., and Blaisdell, J.M., “Retrieval of atmospheric and surface parameters from AIRS/AMSU/HSB data in the presence of clouds,” IEEE Trans. Geoscience and Remote Sensing, 41, 390-409, doi: 10.1109/TGRS.2002.808236 (2003).

Susskind, J., Barnet, C., Blaisdell, J., Iredell, L., Keita, F., Kouvaris, L., Molnar, G., and Chahine, M., “Accuracy of geophysical parameters derived from Atmospheric Infrared Sounder/Advanced Microwave Sounding Unit as a function of fractional cloud cover,” J. of Geophys. Res., 111, D09S17, doi:10.1029/2005JD006272 (2006).

Susskind, J, Blaisdell, J.M., Iredell, L. and Keita, F., “Improved temperature sounding and quality control methodology using AIRS/AMSU data: The AIRS Science Team Version-5 Retrieval Algorithm,” IEEE Trans. on Geoscience and Remote Sensing, Issue: 99, doi: 10.1109/TGRS.2010.2070508, 1-15 (2011).

Susskind, J., Molnar, G., Iredell, L., Loeb, N.G., “Interannual variability of outgoing longwave radiation as observed by AIRS and CERES,” J. Geophys. Res. 117, D23107 doi:10.1029/2012JD017997 (2012)

Susskind, J., Blaisdell, J.M., and Iredell, L. "Improved methodology for surface and atmospheric soundings, error estimates, and quality control procedures: the atmospheric infrared sounder science team version-6 retrieval algorithm." *Journal of Applied Remote Sensing* 8.1 (2014): 084994, doi:10.1117/1.JRS.8.084994.

Susskind, J., Lee, J.N., Iredell, L, and Loeb, N.G., “Diurnal Differences in OLR Time Series and Climatologies”, J. of Geophys. Res., 2018a (ready for submission).

Susskind, J., Lee, J.N., Iredell, L, and Loeb, N.G., “Diurnal Differences in OLR Anomaly Time Series and Correlations with El Niño”, J. of Geophys. Res., 2018b (ready for submission).

Revercomb, H., Strow, L., Braun, J., Garcia, R., Gumley, L., Knuteson, R., Krenzke, E., Martin, G., Motteler, H., Phillips, C., Quinn, G., Taylor, J., and Tobin, D. NASA SNPP Cross Track Infrared Sounder (CrIS) Level 1B Delta Algorithm Theoretical Basis Document (ATBD), May 2017.

Rosenkranz, P., Retrieval of temperature and moisture profiles from AMSU-A and AMSU-B measurements, IEEE, 39, 2429, 2000.

Strow, L.L., H.E. Motteler, R.G. Benson, S.E. Hannon and De Souza-Machado, S., Fastcomputation of monochromatic infrared atmospheric transmittances using compressed look-up tables. J. Quant. Spectrosc. Radiat. Transfer v.59 p.481-493,1998.

Tian, B., E. J. Fetzer, B. H. Kahn, J. Teixeira, E. Manning, and T. Hearty, Evaluating CMIP5 Models using AIRS Tropospheric Air Temperature and Specific Humidity Climatology, J. Geophys. Res. Atmos., 118, 114–134, doi:10.1029/2012JD018607, 2013.